nature neuroscience

ARTICLES

https://doi.org/10.1038/s41593-018-0317-8

State-dependent encoding of sound and behavioral meaning in a tertiary region of the ferret auditory cortex

Diego Elgueda[1,2], Daniel Duque[1,3], Susanne Radtke-Schuller[1], Pingbo Yin[1], Stephen V. David[4], Shihab A. Shamma[1,2,5] and Jonathan B. Fritz[1,2*]

In higher sensory cortices, there is a gradual transformation from sensation to perception and action. In the auditory system, this transformation is revealed by responses in the rostral ventral posterior auditory field (VPr), a tertiary area in the ferret auditory cortex, which shows long-term learning in trained compared to naïve animals, arising from selectively enhanced responses to behaviorally relevant target stimuli. This enhanced representation is further amplified during active performance of spectral or temporal auditory discrimination tasks. VPr also shows sustained short-term memory activity after target stimulus offset, correlated with task response timing and action. These task-related changes in auditory filter properties enable VPr neurons to quickly and nimbly switch between different responses to the same acoustic stimuli, reflecting either spectrotemporal properties, timing, or behavioral meaning of the sound. Furthermore, they demonstrate an interaction between the dynamics of short-term attention and long-term learning, as incoming sound is selectively attended, recognized, and translated into action.

To understand the meaning of sounds, we learn to associate their acoustic features with their behavioral context and link them to appropriate audiomotor responses. Once associative learning has taken place, rapid task-dependent plasticity during active listening may enhance listeners' ability to recognize and respond to relevant incoming sounds by adaptively reshaping auditory cortical filter properties.

Research in visual and somatosensory associative cortices has shown their key role in complex object recognition and perception[1–3], formation of learned categorical representations[4–6], multisensory integration, memory[7], and decision-making[8,9]. However, with a few notable exceptions[10–13], most neurophysiological studies of the auditory cortex in behaving animals have focused on the primary auditory cortex (A1) rather than higher-order auditory cortical areas.

To investigate the contributions of nonprimary auditory cortex to sound processing, we have chosen the ferret, which has become an increasingly valuable animal model to study the neurobiology of auditory behavior and hearing[14]. In previous studies, we have described how task engagement induces rapid plasticity in the primary auditory cortex (A1) and in tonotopically organized secondary or 'belt' areas in the ferret auditory cortex (posterior pseudosylvian field (PPF) and posterior suprasylvian field (PSF) in Fig. 1b). The neural representation of sound can be partially transformed in these areas to incorporate behavioral and contextual information[11,15–17]. We have also characterized a task-dependent, gated representation of behaviorally salient sounds in the non-tonotopic dorsolateral frontal cortex (dlFC)[18].

Based on this earlier work, we conjectured that (1) there are tertiary auditory cortical areas between secondary areas and the frontal cortex where the transformation from sound representation to behavioral meaning is more extensively developed than in lower cortical areas, (2) long-term task learning permanently shapes neuronal responses in these higher areas, a change that should be evident even during task-free (or 'passive') conditions. We also predicted that neurons in higher auditory areas would (3) display strong attention effects that would amplify long-term changes in the representation of task-relevant stimuli during task performance, (4) would show response timing linking auditory inputs to reward and motor responses.

Previous studies have shown that the ferret auditory cortex is composed of multiple acoustically sensitive adjoining areas in the ectosylvian gyrus of the temporal lobe[19,20]. Current maps of ferret auditory cortex include nine distinct cortical areas, six of which (A1, anterior auditory field (AAF), PPF, PSF, anterior dorsal field (ADF), anterior ventral field (AVF)) have been physiologically identified and described previously[19]. One field whose function has not been studied previously, the ventral posterior (VP) area, lies in a ventral region in the posterior ectosylvian gyrus (PEG), and its anatomical connectivity makes it a good candidate for a tertiary auditory field[20–23].

To test these hypotheses concerning sound encoding in the tertiary auditory cortex, we recorded responses under multiple active task and non-task (passively listening) conditions in the rostral region of VP (VPr in Fig. 1a,b)[11,20,21,23]. Partly because of its extreme lateral location and limited accessibility for surface recordings, VP has remained one of the least studied areas of the ferret auditory cortex. In this study , we describe how VPr neurons exhibit striking state- and context-dependent changes in auditory responses and encode non-acoustical sound features, such as associated behavioral

[1]Institute for Systems Research, Department of Electrical and Computer Engineering, University of Maryland, College Park, MD, USA. [2]Neuroscience and Cognitive Science Program, University of Maryland, College Park, MD, USA. [3]Institut d'Investigacions Biomèdiques August Pi i Sunyer , Barcelona, Spain. [4]Oregon Hearing Research Center, Oregon Health and Science University, Portland, OR, USA. [5]Laboratoire des Systèmes Perceptifs, École Normale Supérieure, Paris, France. *e-mail: ripple@isr.umd.edu

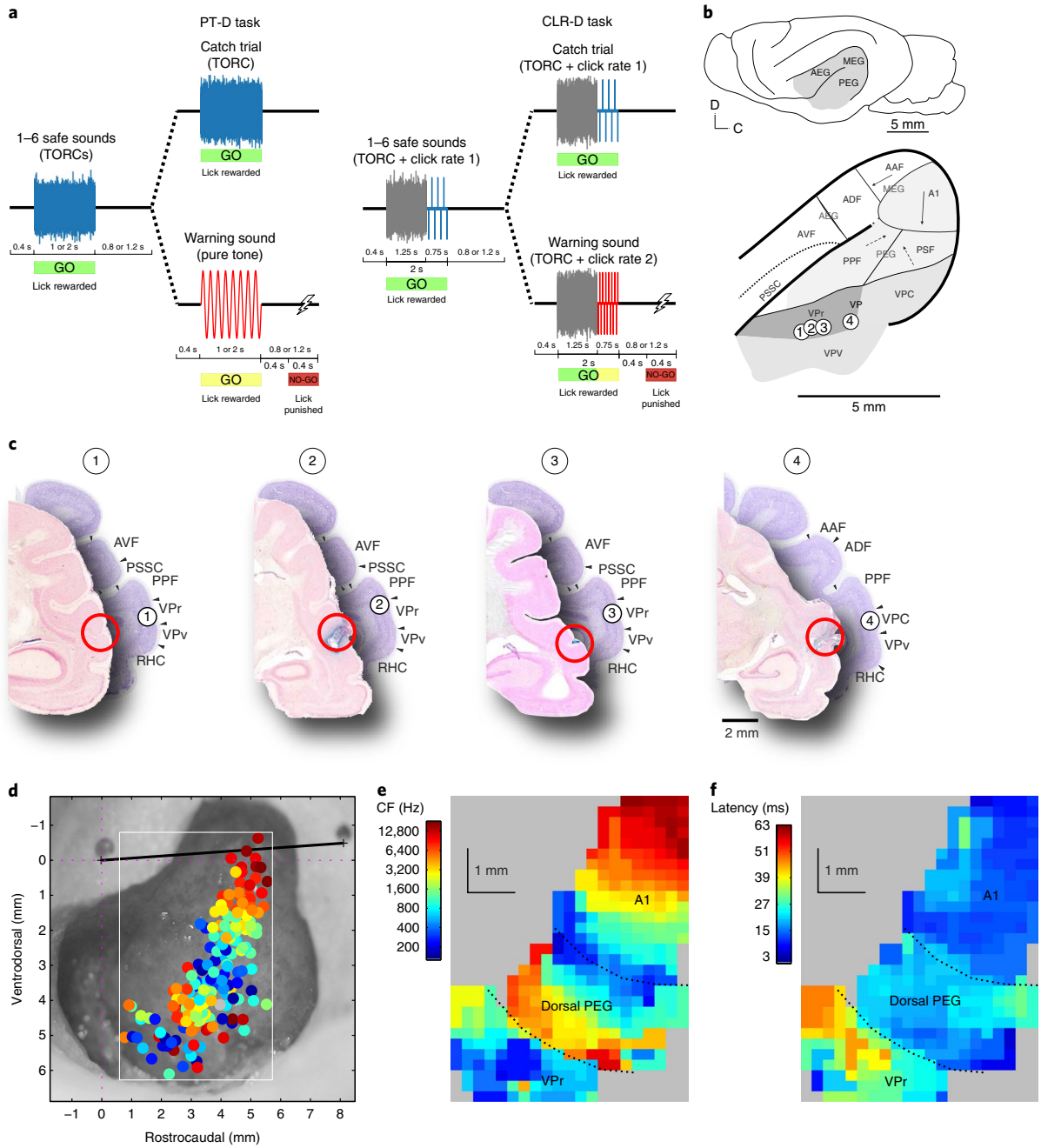

Fig. 1 | Behavioral task design and location of neurophysiological recordings. a, PT-D and CLR-D tasks. Both tasks used a conditioned avoidance framework, in which animals were trained to freely lick water from a spout during the presentation of safe sounds and to refrain from licking for a time window of 400–800 ms after the offset of a warning sound to avoid a mild tail shock. In the PT-D task, safe sounds were a class of 30 similar TORCs and warning sounds were pure tones. In the CLR-D task, both safe and warning sounds were composed of 1.25-s TORCs followed by 0.75-s click-trains of differing rates; animals were trained to discriminate between safe and warning click-trains of different rates. For both tasks, on a given trial, a random number of safe sounds (1–6) were followed by a warning sound. In catch trials, there were no warning sounds. In each behavioral session (comprised of ~40 trials), the warning tone frequencies (for PT-D), as well as the safe and warning click rates (for CLR-D), were varied and chosen after initial characterization of neuronal tuning. TORC and tone durations were either 1 or 2 s. Interstimulus silences were either 0.8 or 1.2 s. **b**, Location of fields in the ferret auditory cortex. Primary areas A1 and AAF are located in the medial ectosylvian gyrus (MEG) and display a clear tonotopic gradient, shown by a solid arrow. Two secondary areas in the dorsal posterior ectosylvian gyrus PEG (posterior pseudosylvian field, or PPF, and posterior suprasylvian field, or PSF) are lateroventrally adjacent to A1 and display coarser and more variable tonotopic gradients (dashed arrow). Tertiary area VP, subdivided into rostral, caudal, and ventral fields (VPr, VPc, and VPv, respectively), displays broad spectral tuning and no apparent tonotopy. The numbers indicate the location of neuroanatomical markers placed in the vicinity of recording locations in four mapped hemispheres. **c**, Coronal sections in four hemispheres show recording locations in VPr and their corresponding atlas section locations (Atlas[21] section positions in mm relative to the occipital crest, marking the caudal end of the ferret skull: (1) −18 mm; (2) −17.7 mm; (3) −17.7 mm; (4) −16.5 mm). AEG, anterior ectosylvian gyrus; PSSC, pseudosylvian sulcus cortex; RHC, rhinal cortex. The projected locations of marks from the map in **b** are depicted with circled numbers. **d**, Characteristic frequencies (CFs) recorded in one ferret, where each dot color corresponds to the mean CF across all neurons recorded in one electrode penetration. **e**, These CF measurements were used to generate a map, which displays three functionally distinct areas corresponding to A1, dorsal PEG area PPF, and VPr. **f**, Increasing response latencies in the three cortical maps, measured from the same recordings, also suggest three distinct stages in cortical processing from MEG to PEG.

meaning and task timing. These results are consistent with all four of the conjectures above.

Results

Neurophysiological mapping and neuroanatomical location. We mapped the basic tuning properties of VPr using single-unit activity in six animals during passive presentation of pure tone, click-train, and broadband rippled noise stimuli (see Methods).

We marked the location of VPr recordings and confirmed that they were ventral and anterior to area PPF (Fig. 1b,c; sites are labeled with electrolytic lesions, electrolytic deposits of iron, or injections of neuroanatomical tracer). All microelectrode penetrations into VPr followed a 30-degree angle relative to the sagittal plane. The neuronal depths of >90% of our VPr recordings were close to the cortical surface, within the first 500 µm of the first spikes recorded as electrodes entered the brain (Supplementary Fig. 1). The location of each recording site was also registered with a ferret brain atlas[21] (Fig. 1c). VPr spans an area 1–2 mm below and ventral to high-frequency PPF (Fig. 1d,e) and ventral to the lower lip of the pseudosylvian sulcus (PSS) and is physiologically characterized by a drastic change in the tonotopic map (Fig. 1e) and an increase in response latency (Fig. 1f).

Response properties in VPr. The basic auditory tuning properties of single units in VPr are contrasted with previously collected responses from A1 and dorsal PEG (Fig. 2). The distribution of tuning properties is consistent with neuroanatomical evidence that VPr is a later processing stage in the auditory pathway, after A1 and dorsal PEG[20]. Compared to earlier areas, VPr neurons display longer mean latency (Fig. 2a; VPr: $n=583$ neurons, 37.71 ± 1.78 ms; dorsal PEG: $n=1{,}125$ neurons, 24.45 ± 0.57 ms; A1: $n=2{,}309$ neurons, 15.57 ± 0.88 ms). We found significant differences in tone response latency ($\chi^2=862.83$, $P<0.0001$, d.f. = 2, Kruskal–Wallis test), where VPr significantly differed from A1 (Tukey's honestly significant difference (HSD) effect size ($\text{mean}_{(A1)}-\text{mean}_{(VPr)}$) = −1,265.8, 95% confidence interval (CI) = (−1,388.9, −1,142.7), $P=0$) and dorsal PEG (effect size ($\text{mean}_{(\text{dorsal PEG})}-\text{mean}_{(VPr)}$) = −341.8, 95% CI = (−477.3, −206.3), $P=0$).

Neurons in VPr also have broader mean frequency tuning bandwidth (Fig. 2b; VPr: $n=635$ neurons, 1.77 ± 0.05 octaves (oct); dorsal PEG: $n=1{,}202$ neurons, 1.4 ± 0.05 oct; A1: $n=2{,}594$ neurons, 1.07 ± 0.04 oct; $\chi^2=499.16$, $P<0.001$, d.f. = 2, Kruskal–Wallis test). Mean VPr bandwidth was significantly greater than A1 (effect size = −1,190.9, 95% CI = (−1323.6, −1,058.2), $P=0$) and dorsal PEG (effect size = −630.7, 95% CI = (−777.8, −483.7), $P=0$).

VPr neurons also display weaker overall following of complex synthetic sounds (Fig. 2c; mean signal-to-noise ratio (SNR); VPr: $n=516$ neurons, 0.34 ± 0.05; dorsal PEG: $n=986$ neurons, 0.55 ± 0.1; A1: $n=2{,}399$ neurons, 0.73 ± 0.08; $\chi^2=291.06$, $P<0.001$, d.f. = 2, Kruskal–Wallis test). The SNR of the VPr responses was significantly lower than A1 (effect size = 816.24, 95% CI = (688.15, 944.33), $P=0$) and dorsal PEG neurons (effect size = 329.55, 95% CI = (186.13, 4,472.97), $P=0$).

For neurons whose responses followed the stimulus, spectrotemporal receptive fields (STRFs) were more complex, as indicated by their sparseness index—the peak STRF magnitude divided by the s.d. across the STRF bins (Fig. 2d; VPr: $n=180$ neurons, 0.44 ± 0.09; dorsal PEG: $n=472$ neurons, 1.35 ± 0.09; A1: $n=1{,}664$ neurons, 2.24 ± 0.13; $\chi^2=291.06$, $P<0.001$, d.f. = 2). VPr showed lower STRF sparseness than A1 (effect size = 777.47, 95 CI = (655.48, 899.45), $P=0$) and dorsal PEG (effect size = 466.29, 95% CI = (330.18, 602.4), $P=0$).

Thus, VPr occupies an intermediate stage in auditory processing, resembling the earlier stages by its tuned responses to tones and occasional phase locking to modulated stimuli, which allow for STRF measurements in some neurons (in VPr, only 27.3% (180/658) of cells have SNR > 0.2, compared to 35.3% in dorsal PEG (472/1,337) and 60% in A1 (1,644/2,740)). However, VPr is also similar to dlFC in its relatively weak auditory responsiveness during passive sound presentation[18], its often poorly defined tuning, and long response latencies (examples in Fig. 3a,c and Supplementary Figs. 2, 3).

Response modulation during task performance. Responses in VPr changed dramatically during task performance to reflect the behavioral valence of the stimuli as positively (GO) or negative rewarded (NO-GO) sounds. A total of 367 single units were recorded in 4 trained ferrets, before (pre-passive), during, and after (post-passive) performance of two distinct conditioned avoidance tasks, learned before the recordings[15]. The tasks were: (1) tone versus noise discrimination task ('pure tone detection', PT-D); and (2) click-rate discrimination (CLR-D) task (Fig. 1a). In both tasks, the animals listened to a sequence of reference 'safe' sounds (broadband rippled noise—temporally orthogonal ripple combinations (TORCs)—in PT-D or a range of click-train rates in CLR-D) during which the animal could safely lick a waterspout for reward. The sequence of safe sounds ended either with a final safe sound (catch trials) or with a 'warning' target sound (tone in PT-D and a different click rate in CLR-D) that alerted the animals to stop licking 400 ms after target offset to avoid a mild shock. For different CLR-D animals, warning click rates were either lower or higher than that of safe rates. During each recording session, animals often engaged in blocks of two or more tasks with different stimuli.

Examples of single-unit responses in VPr during behavior are shown in Fig. 3a, d. In the majority of units, engagement in behavior rapidly induced a substantial change in peristimulus time histogram (PSTH) responses to warning stimuli, and a lesser change for safe stimuli (Fig. 3a,d). In the extreme, some units were behaviorally gated and showed virtually no response to task-related sounds unless the animal was engaged in behavior (Supplementary Fig. 3). Details of changes varied greatly from cell to cell, reflecting the specific type of response (for example, onset, sustained, or offset). Nevertheless, the patterns of responses to warning and safe stimuli in the population average (Fig. 3b,e) remained largely similar for both tasks despite the different stimuli (TORCs/tones versus TORC-click-trains—average responses to 30 different TORCs and multiple click-train rates). Population averages (PSTHs) to safe (rate 1) and warning (rate 2) click rates were averaged across different click rate trains for animals trained with either low or high click rates as warning stimuli (see Supplementary Fig. 4). Thus, on average, there was a large enhancement in the responses to the class of NO-GO warning stimuli (that is, tone or target click-train) during behavior, compared to smaller changes in the class of safe stimulus responses.

Task-dependent response changes were measured by the difference in normalized firing rates ($\Delta\text{nFR}_{(B-P)}$) between behaving and passive conditions (Fig. 3c,f). This differential change increased the contrast between safe and warning responses, much greater in magnitude but in a similar direction to changes reported earlier in secondary auditory areas[11]. Behavioral state could alter neuronal responses to a given stimulus from onset to sustained (Fig. 3a, lower panel) or even gate VPr neuronal responses so that they only occurred in the active state (Supplementary Fig. 3).

The relationship of VPr responses to behavior is illustrated (Fig. 3b,e), juxtaposing the population lick probability for safe and warning (hits only) sounds to the population neural response for the two tasks. Lick probability for the safe sounds remains constant during and after these stimuli. However, lick probability for the warning sound is clearly depressed, not only during the stimulus, but also poststimulus, and until the end of the shock window (shaded area). A comparison with the population neural PSTH

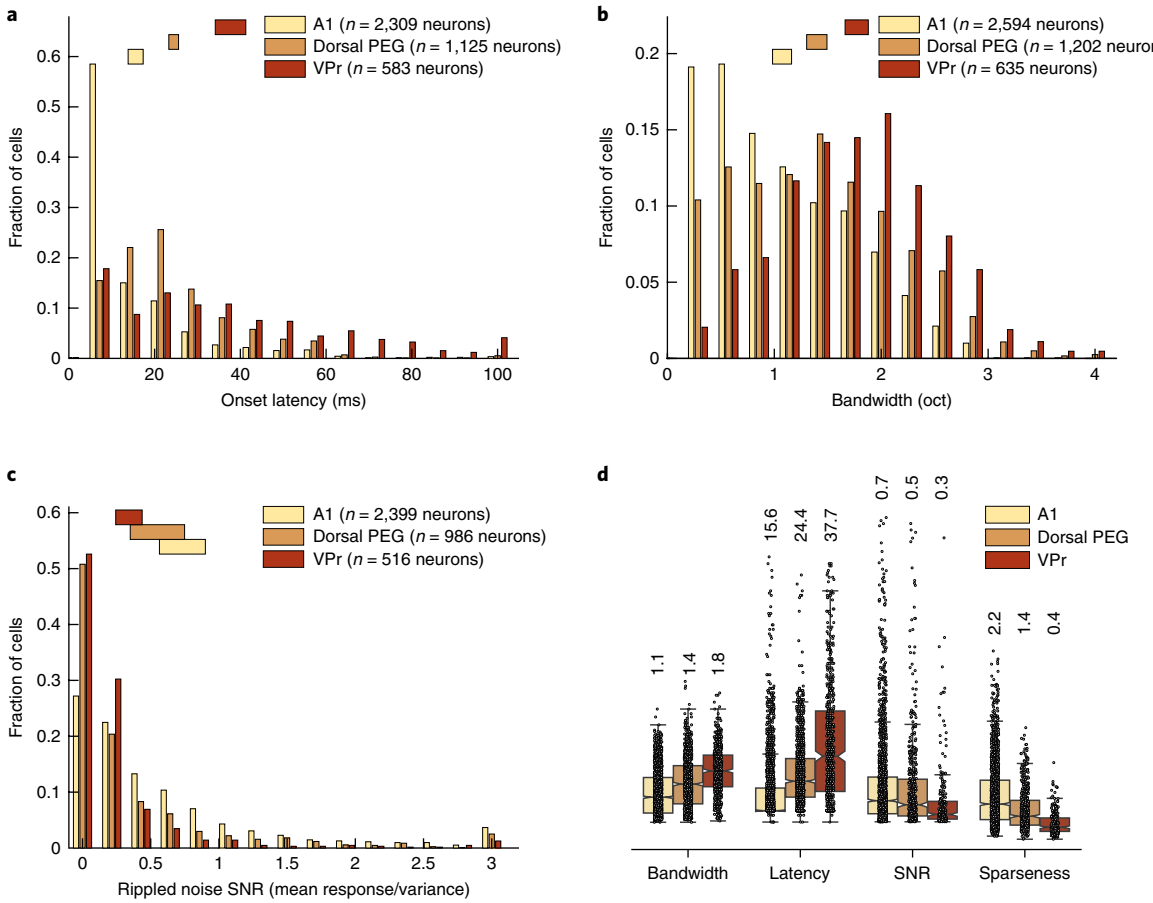

Fig. 2 | Comparison of the tuning properties of the A1, dorsal PEG, and VPr areas. Tuning parameters were measured from the responses to tones and TORCs and their resultant PSTHs and STRFs during passive listening. The bars at the top of the histograms in **a**–**c** indicate mean ± s.e.m. in each area (A1, light tan; dorsal PEG, orange; VPr, red). **a**, Response latency measured from the PSTH response to random tones, measured as the earliest time bin after tone onset significantly modulated from baseline spontaneous activity ($P < 0.05$, two-sided jack-knifed t test; mean ± s.e.m. A1: 15.57 ± 0.88; dorsal PEG: 24.45 ± 0.57; VPr: 37.71 ± 1.78). All neurons with measurable auditory responses and significant latencies were included (A1: $n = 2{,}309/2{,}740$ neurons; dorsal PEG: $n = 1{,}125/1{,}337$ neurons; VPr: $n = 635/658$ neurons; $P < 0.05$, two-sided jack-knifed t test). **b**, Bandwidth of frequency tuning, measured as octaves at the half-height of tuning curves constructed by fitting a Gaussian function to average tone responses (mean ± s.e.m., A1: 1.07 ± 0.04; dorsal PEG: 1.4 ± 0.05; VPr: 1.77 ± 0.05). All neurons with measurable auditory responses and significant bandwidth values were included (A1: $n = 2{,}597/2{,}740$ neurons; dorsal PEG: 1,202/1,337 neurons; VPr: 635/658 neurons; $P < 0.05$, two-sided jack-knifed t test). **c**, SNR of neural responses to TORC stimuli measured as trial-to-trial phase locking to TORC sounds (mean ± s.e.m., A1: 0.73 ± 0.08; dorsal PEG: 0.55 ± 0.1; VPr: 0.34 ± 0.05). All neurons with SNR values > 0 were measured (A1: $n = 2{,}399/2{,}740$ neurons; dorsal PEG: $n = 986/1{,}337$ neurons; VPr: $n = 516/658$ neurons). **d**, Summary of mean (± s.e.m.) tuning parameters measured in A1, dorsal PEG, and VPr. Sparseness: mean STRF sparseness index, measured as the ratio between peak and mean magnitudes measured from STRF estimates (mean ± s.e.m., A1: 2.24 ± 0.13; dorsal PEG: 1.35 ± 0.09; VPr: 0.44 ± 0.09). For this measure, only neurons with phase locking (SNR > 0.2, as measured in **c**) were considered (A1: $n = 1{,}664/2{,}740$ neurons; dorsal PEG: $n = 472/1{,}337$ neurons; VPr: $n = 180/658$ neurons; see Methods).

for the two tasks illustrates that the timing of the increased neural responses to the warning stimuli parallels decreases in the behavioral lick response.

Response transformations from A1 to dorsal PEG, VPr, and dlFC. To gain a broader view of VPr in the broader cortical network, we compared population PSTH responses in A1, dorsal PEG, and dlFC during pre-passive and behavior epochs for both PT-D and CLR-D tasks (Fig. 4). PT-D data from the A1, dorsal PEG, and dlFC of 14 additional ferrets[11,15,17,18] were reanalyzed and added to the PT-D averages to provide a larger sample (see Methods). We measured stimulus contrast as the difference between warning and safe responses ($\Delta nFR_{(W\text{-}S)}$, baseline subtracted, normalized amplitude PSTH. PT-D: 0.1–0.45 s after sound onset; CLR-D: 0.3–1 s after TORC offset/click-train onset) for both passive and behaving conditions (PSTHs in Fig. 4a,b, contrasting distributions in Fig. 6).

There are several notable findings in the comparison of population average responses across areas and tasks. First, the overall pattern of enhanced contrast ($\Delta nFR_{(W\text{-}S)}$) between warning and safe responses during behavior is similar in both tasks. Overall changes in contrast from one cortical area to another for the two tasks are remarkably similar at the population level, despite considerable differences between their stimuli. This points to the primacy of behavioral meaning of the stimuli in the tasks (as GO or NO-GO) rather than their acoustic properties in determining the nature of VPr responses. At a single-cell level, many VPr neurons (150/367 = 41%) showed similar enhanced target responses in both PT-D and CLR-D tasks (Supplementary Fig. 5).

Second, contrast enhancement between warning and safe ($\Delta nFR_{(W\text{-}S)}$) gradually increased across areas during behavior compared to the pre-passive state (left versus right columns in Fig. 4a,b). We interpret this to indicate a progressively larger weight given to

the behavioral distinction between NO-GO and GO stimuli in higher cortical areas. The overall change in contrast in A1 is much smaller than in dorsal PEG (for example, CLR-D task of Fig. 4b). In fact, the average warning tone response in A1 during PT-D (Fig. 4a) is actually smaller than the responses to the safe TORCs. This reversal probably reflects the sensitivity of A1 neurons to tone frequency. In many experiments, recordings were made simultaneously from neurons with different frequency tuning. Hence the target tone frequency could not be optimized to deliver the enhancements described earlier in studies where the warning tone was often placed close to the best frequency to achieve maximal plasticity[11,15].

We compared responses in different areas using a three-way repeated-measures analysis of variance (ANOVA) (see Methods). In the PT-D task (A1 $n=71$; dorsal PEG $n=199$; VPr $n=251$; dlFC $n=138$ neurons) the repeated-measures ANOVA for the response difference ($\Delta nFR_{(W\text{-}S)}$) yielded significant main effects for area ($F=8.91$; $P<0.0001$) and task condition (passive or behaving, $F=11.52$; $P=0.0007$). Tukey's HSD test confirmed that response differences are smaller in A1 compared to the other areas (A1-dorsal PEG $=2.759$, 95% CI $=(1.201, 4.316)$, $P<0.0001$; A1-VPr $=2.944$, 95% CI $=(1.418, 4.470)$, $P<0.0001$; A1-dlFC $=2.202$, 95% CI $=(0.580, 3.823)$, $P=0.0028$). A t-test confirmed that response differences are larger when the animal is engaged in the task (passive-behavior $=0.571$, 95% CI $=(0.247,0.894)$, $t=-3.468$, $P=0.0006$). The analysis also yielded a significant area versus behavior interaction ($F=2.64$; $P<0.0487$), suggesting that the effect of engagement on the response depends on the area. Tukey's HSD post hoc analysis again confirmed that behavior enhances response contrast ($\Delta nFR_{(W\text{-}S)}$) in VPr and dlFC (VPr passive-behavior $=0.903$, 95% CI $=(0.135, 1.670)$, $P=0.0089$; dlFC passive-behavior $=1.120$, 95% CI $=(0.171, 2.070)$, $P=0.0086$), but not in A1 or dorsal PEG (A1 passive-behavior $=0.003$, 95% CI $=(-1.356, 1.363)$, $P=1$; dorsal PEG passive-behavior $=0.213$, 95% CI $=(-0.616, 1.044)$, $P=0.994$). Altogether, this analysis suggests that VPr neurons show contrast enhancement that more closely resembles dlFC than dorsal PEG.

In the CLR-D task (A1 $n=57$; dorsal PEG $n=60$; VPr $n=266$; dlFC $n=38$ neurons), the repeated-measures ANOVA yielded a significant main effect for task condition ($F=29.47$; $P<0.0001$). A t-test confirmed that response differences are larger during the active behavior condition (passive-behavior $=1.010$, 95% CI $=(0.701, 1.497)$, $t=5.429$, $P<0.0001$). The analysis also yielded a significant area versus task condition interaction ($F=2.74$; $P<0.0429$). Post hoc Tukey's HSD analysis confirmed that behavior enhances the response contrast between warning and safe click-trains in VPr and dlFC (VPr passive-behavior $=0.798$, 95% CI $=(0.213, 1.382)$, $P=0.001$; dlFC passive-behavior $=2.146$, 95% CI $=(0.551, 3.740)$, $P=0.0013$), but not in A1 or dorsal PEG (A1 passive-behavior $=0.312$, 95% CI $=(-0.979, 1.603)$, $P=0.999$; dorsal PEG passive-behavior $=1.142$, 95% CI $=(-0.097, 2.381)$, $P=0.096$). These findings suggest that a better representation of click-trains in A1 and dorsal PEG—when the animal is engaged in a behavioral task—may be used to generate more highly differentiated behavioral percepts in higher-order areas of the auditory and frontal cortices.

The relation of VPr responses to motor action (licking) was analyzed by cross-correlating spikes with licks[18] (see Methods). Based on this analysis, we found that 37% of VPr neurons ($N=93/251$ neurons tested in the PT-D task) had a significant motor component in their activity. However, behavior-induced changes in sound-evoked activity were independent of these motor effects.

Fig. 3 | VPr neurons enhance the contrast between responses to safe and warning stimuli during behavior. a, Raster plots and PSTH (mean firing rate ± 1 s.e.m.) responses of two VPr neurons to classes of task stimuli before (pre-passive), during (behavior), and after (post-passive) performance of the PT-D task. The shaded areas indicate the duration of safe (blue) and warning (red) sounds. The green dashed lines indicate sound onset and offset; the gray shaded areas and red dashed lines indicate the duration of the behavioral response time window. Left (pre-passive): the top single unit had a small onset response with a relatively long latency (175 ms). A completely different response type is seen in the lower unit, which has a small onset response but then builds up, reaching a maximum response after 0.5 s, and then gradually decays as the tone continues. The responses to TORCs (class of 30 different TORCs) are very weak and become gradually more suppressed over time. Middle (behavior): during behavior, unit responses change dramatically, becoming substantially enhanced especially for warning stimuli, relative to the much weaker safe TORC responses. Right (post-passive): during the post-passive period, the changes subside across variable timescales. For the top unit, warning responses remain somewhat enhanced compared to the pre-passive state, whereas for the lower unit behaviorally induced enhanced responses vanish rapidly. **b**, Population average PSTH (mean firing rate ± 1 s.e.m.) from all VPr units significantly modulated during PT-D behavior ($n=251$ neurons). The gray dashed lines show sound onset and offset. The gray shaded areas and red dashed lines indicate the duration of the behavioral response window (RW). Left: responses to the safe TORCs are largely suppressed relative to baseline spontaneous activity during the pre-passive period (blue dashed curve), becoming less so during behavior (blue solid curve). The black curve shows the constant lick probability for the safe sounds. Right: Excitatory warning responses in the passive condition (dashed line) become substantially enhanced during behavior (solid line). Note mirror image inverse correlation of the population PSTH with the lick probability curve (black). **c**, Difference in normalized firing rates ($\Delta nFR_{(B\text{-}P)}$) between active and passive conditions for safe TORC stimuli (blue curve) and for warning tone stimuli (red curve) calculated from the data in **b** ($n=251$ neurons). The gray dashed lines show sound onset and offset. The gray shaded areas and red dashed lines indicate the duration of the behavioral RW. **d**, Example raster plots and PSTHs of two units before, during, and after performance of the CLR-D task. The shaded areas indicate the duration of safe (blue) and warning (red) sounds. The green dashed lines indicate sound onset and offset. The gray shaded areas and red dashed lines indicate the duration of the behavioral time RW. Cells exhibit little change in responses to the 30 'neutral' TORC stimuli (0–1.25 s) between behavioral epochs. Despite the completely different acoustic properties of the click-train versus tone stimuli, behavior-induced response changes are similar to those observed in the PT-D task. Thus, warning responses in the pre-passive (red curves and rasters, left) become significantly enhanced relative to the safe responses during behavior (middle), with varied persistence in the post-passive period (right). **e**, Population average PSTH calculated from all VPr units significantly modulated during behavior in the CLR-D task ($n=266$ neurons). The gray dashed lines show sound duration. The gray shaded areas and red dashed lines indicate the duration of the behavioral RW. The large, sustained warning enhancement contrasts with smaller changes in the safe responses. The smaller changes in responses to the neutral TORC stimuli (0–1.25 s) are identical regardless of their attachment to safe or warning stimuli. Note that the population averages for both safe and warning click-trains includes the full range of different click rates used in the CLR-D task (see Supplementary Fig. 2). Note that as in the PT-D task (Fig. 3b), there is no change in licking rate (black curve) during the safe sound or during the behaviorally neutral TORC component of the warning sound. However, as soon as the warning click-train is presented, there is an abrupt decrease in lick rate paralleled by a sharp increase in neural firing rate during active behavior (solid blue curve). Neuronal activity remains high and lick rate stays low throughout the 800-ms poststimulus period. The two mirror image curves come back together after the shock period. **f**, Difference in normalized firing rates ($\Delta nFR_{(B\text{-}P)}$) between active and passive conditions for safe click-rate 1 stimuli (blue curve) and for warning click-rate 2 stimuli (red curve) for population shown in **e** ($n=266$ neurons). The gray dashed lines show sound duration. The gray shaded areas and red dashed lines indicate the duration of the behavioral RW.

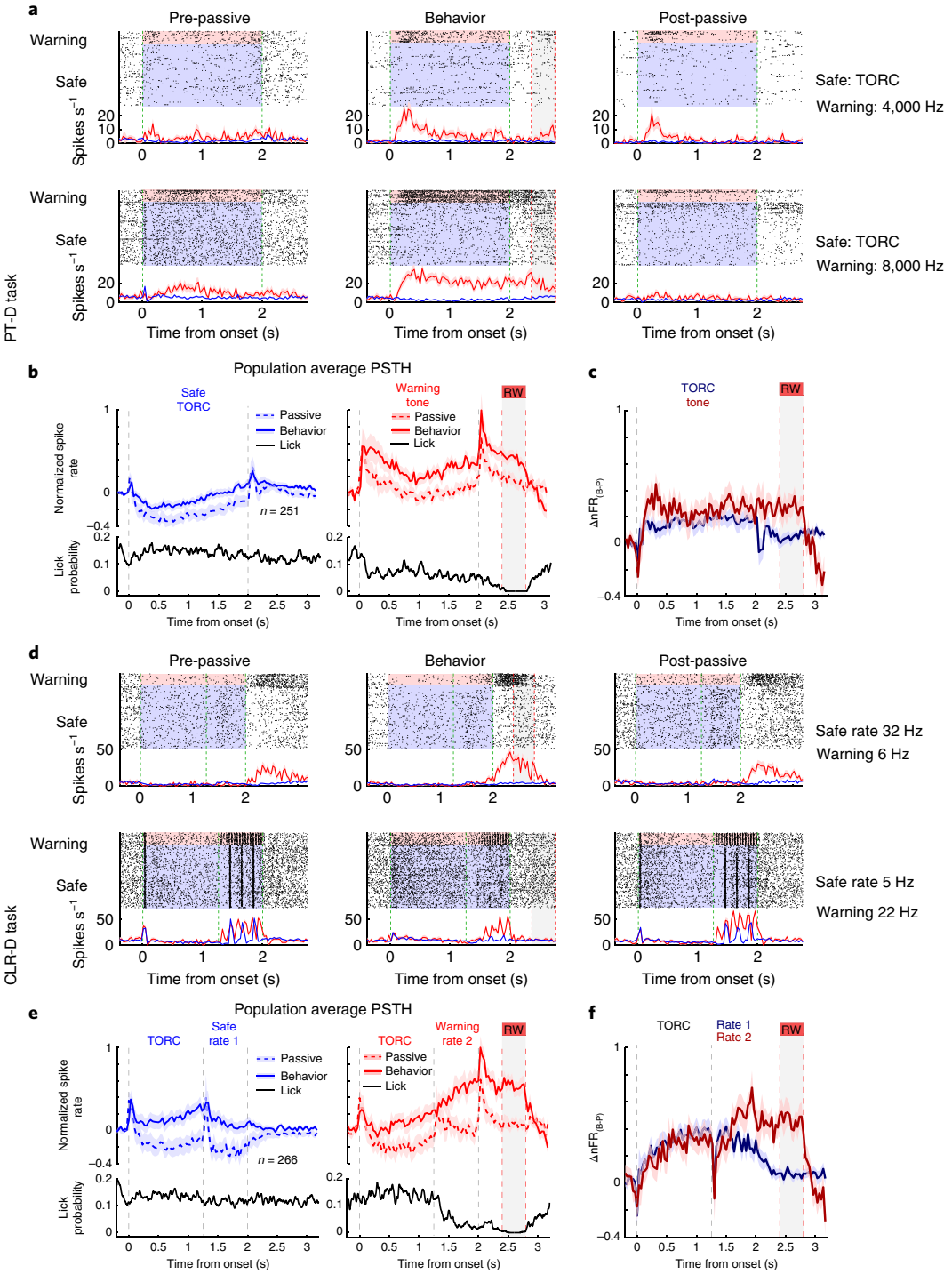

When we subtracted all lick-predicted spike activity from the 37% of VPr neurons with significant motor-related activity, population mean PSTHs did not change significantly (one-way ANOVA, $F = 0.43$, $P = 0.5122$, Supplementary Fig. 6). This analysis also highlights an observation about the prevalence of motor-related activity in VPr. The prevalence of neurons with motor-related activity is 20% in A1 (14/71), 13% in dorsal PEG (26/199), 37% in VPr (93/251), and 20% in dlFC (161/788). Thus, motor-related activity is more common in VPr than in the other auditory cortical areas.

Progressive contrast enhancement exists even in the quiescent state. Previous work on auditory learning in adult animals has shown that the auditory cortex undergoes long-term changes that reflect training on behaviorally relevant sound features[24,25]. Conversely, artificially enhancing neural responses to acoustic stimuli can improve behavioral responses to those stimuli[26–28]. Thus, we predicted that we would observe enhanced contrast between warning and safe responses, not only during behavior, but also during passive listening. We measured warning versus safe contrast during the pre-passive epoch in both tasks and observed that contrast indeed increased from A1 to VPr (Figs. 4 and 5). We note that because of behavioral gating[18], the dlFC is somewhat different from earlier auditory cortical areas, in that it rarely responds to task stimuli during passive listening in the PT-D or CLR-D tasks. We hypothesize that the significant change in contrast effects (from A1 to VPr) during the pre-passive state may reflect the

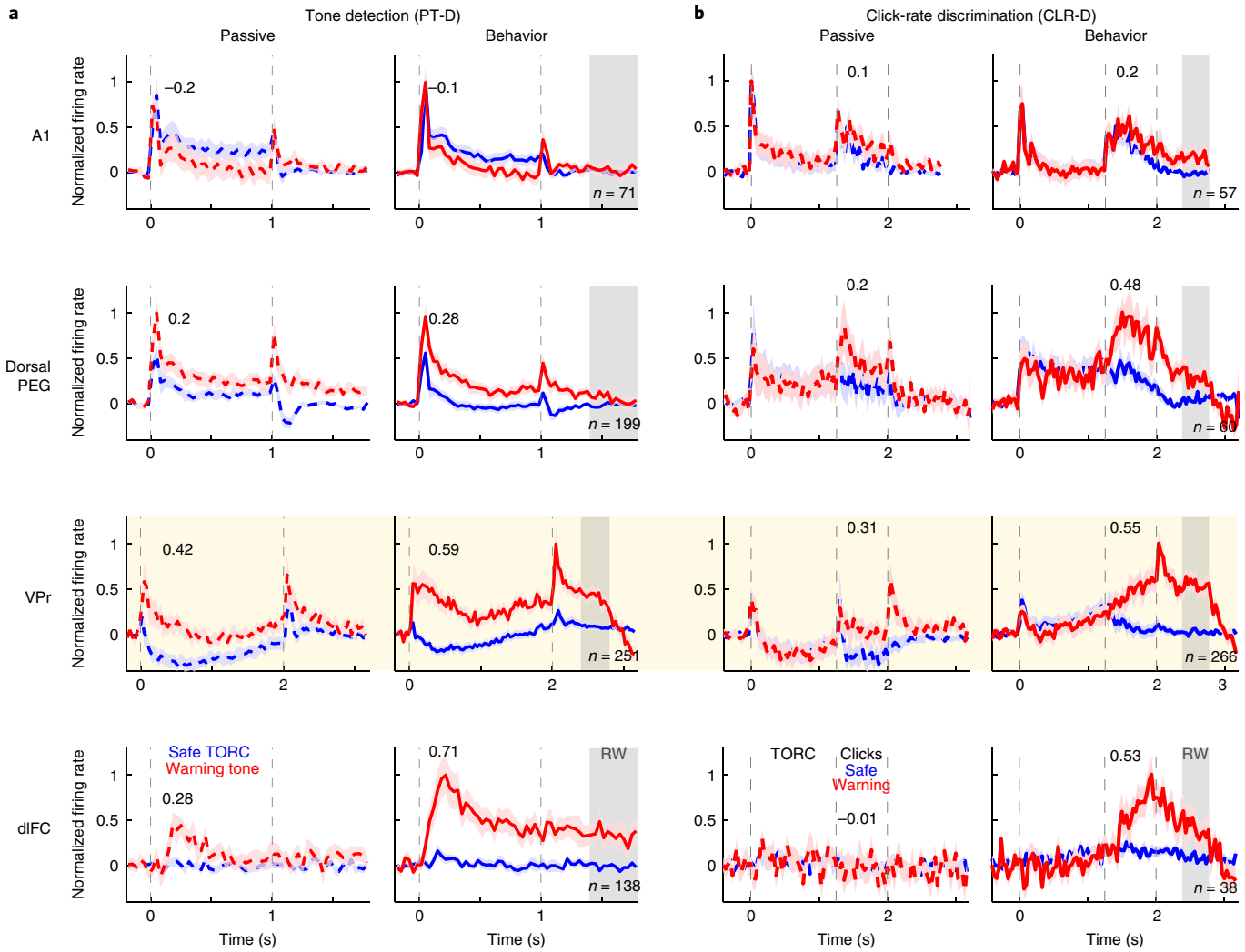

Fig. 4 | Average responses to warning and safe stimuli from the A1, dorsal PEG, VPr, and dlFC areas. a, During PT-D task. **b**, During CLR-D task. In each row, the mean ± s.e.m. time-varying responses to warning (red) and safe (blue) stimuli are compared in pre-passive (left column, dashed curves) and behavior conditions (right column, solid curves). Neural responses were normalized to have the same maximum across behavior conditions before averaging. All cells that exhibited modulated responses during behavior compared to the pre-passive state were included in the averages. The vertical dashed lines indicate sound onset and offset. The gray shaded area indicates the 400-ms behavioral RW during which animals could receive a shock if they continued licking following warning sound offset. The cream shaded area indicates data obtained from VPr. The numbers above curves indicate the contrast between safe and warning sound responses ($\Delta nFR_{(W\text{-}S)}$; see Methods and Fig. 6), measured as the mean difference in normalized firing rate in response to sounds in a time window 0.1–0.45 s from onset (PT-D task) or 0.3–1 s after TORC offset (CLR-D task). PT-D: A1 $n = 71$; dorsal PEG $n = 199$; VPr $n = 251$; dlFC $n = 138$ neurons. CLR-D: A1 $n = 57$; dorsal PEG $n = 60$; VPr $n = 266$; dlFC $n = 38$ neurons.

persistent effects of behavioral training. A consequence of this explanation would be that task-naïve animals should not exhibit any such effects, as we shall demonstrate and discuss.

To summarize, there is a gradual shift toward an enhanced representation of behavioral meaning of task stimuli beginning in the early cortical stages (A1 and dorsal PEG) and increasing toward the higher cortical regions where it becomes clearly manifested in dlFC. VPr is similar to the early auditory cortical areas, responding to both contrasted warning-safe sounds reflecting their acoustic features, such as tone frequency and temporal dynamics. On the other hand, VPr responses also resemble those in dlFC in their state-dependent response changes and selective representation of warning stimuli during behavior.

Behavioral gating in VPr: comparison with responses in dlFC. There is a subset of neurons in VPr that exhibit behaviorally gated responses. They are non-responsive to acoustic stimuli during passive listening but show clear responses to the same sounds during behavior (Supplementary Fig. 3). As mentioned, these behaviorally gated responses in VPr are similar to responses previously observed in dlFC[18]. About 28% of VPr neurons (127/453) showed no response to a variety of passively presented acoustic stimuli (that is, no behavioral task context). However, in active task conditions, only 12% (54/453) were unresponsive. Thus, 16% (73/453) of VPr neurons were behaviorally gated. However, unlike dlFC, a majority (72%) of VPr neurons still display some broad pre-passive responses. Passive responses are largely absent in the dlFC for either of the two tasks, especially for the CLR-D task (Fig. 4). In the dlFC, the small pre-passive responses observed for PT-D may be largely due to persistent enhancement from previous tasks performed in the same recording session[18].

Contrast between warning and safe stimuli is qualitatively different in naïve and trained animals. Since the behavioral meaning of

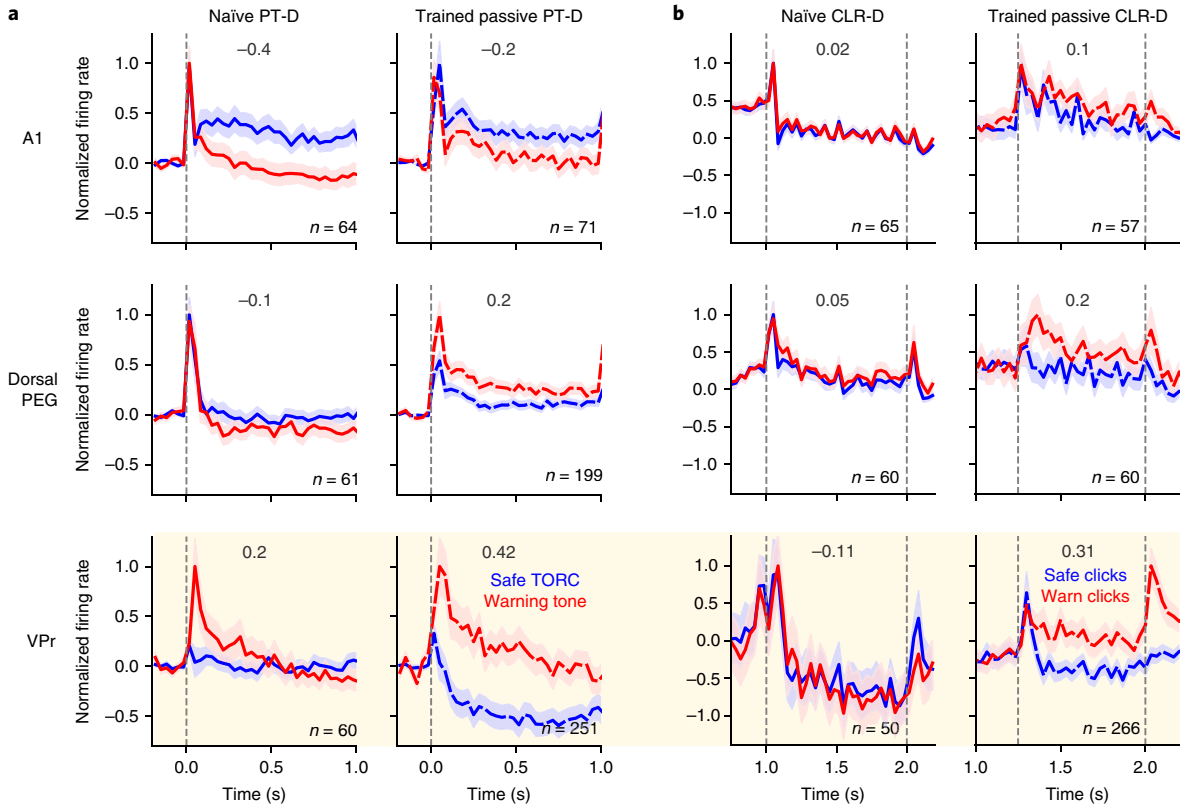

Fig. 5 | Comparison of contrast between safe and warning sounds in naïve and trained animals in three different auditory cortical areas. a, Mean ± s.e.m. normalized firing rates in response to TORCs (blue) and tones (red) in PT-D. The left column displays the responses to the passive presentation of task sounds to a task-naïve animal (A1 $n = 64$; dorsal PEG $n = 61$; VPr $n = 60$ neurons). The right column displays the data acquired during presentation of the PT-D task to trained animals (dashed lines) during the passive state (A1 $n = 71$; dorsal PEG $n = 199$; VPr $n = 251$ neurons). The vertical gray lines indicate sound onset. The cream shaded area indicates the VPr responses. **b**, Responses to safe (blue) and warning (red) click-trains recorded while passively presenting the CLR-D task sounds to a task-naïve ferret (left; A1 $n = 65$; dorsal PEG $n = 60$; VPr $n = 50$ neurons) and trained ferrets (right; A1 $n = 57$; dorsal PEG $n = 60$; VPr $n = 266$ neurons). Even in the behaviorally quiescent listening condition in trained animals (dashed lines), VPr neurons display a greater contrast between safe and warning sounds than is observed in a naïve animal. This contrast is further increased during task performance (see Fig. 4). The vertical gray lines indicate click-train onset and offset. The numbers above the curves display the mean safe and warning response contrast ($\Delta nFR_{(W\text{-}S)}$; see Methods and Fig. 6).

the warning and safe stimuli emerges as a result of behavioral training on the GO/NO-GO tasks, we conjectured that these two classes of sound might leave a trace in higher cortical sensory regions reflecting their meaning, even when the animal was not engaged in performing the task. The strong response contrast between warning and safe stimuli ($\Delta nFR_{(W\text{-}S)}$) during passive listening suggests that this is the case (Fig. 4). However, if behavioral training causes these long-term changes, the difference between warning and safe responses should be less pronounced and should not increase in the higher auditory areas of task-naïve animals. To test this prediction, we recorded the responses to task stimuli in A1, dorsal PEG, and VPr of a task-naïve animal (Fig. 5a,b). For the PT-D stimuli, A1 responses in the naïve and trained animals are quite similar and they clearly discriminate between tones and TORCs. These different responses faithfully reflect differences in the stimuli. For the CLR-D stimuli, there is no difference in the A1 population response to low- and high-rate click-trains in either naïve or trained animals. Enhanced contrast (compared to naïve animals) begins to emerge in the trained animals in dorsal PEG, where the warning response significantly exceeds the safe stimuli response. The contrast becomes even clearer in VPr, where the GO/NO-GO behavioral meaning they have acquired during training is clearly manifested in both pre-passive and active behavior conditions in VPr (Fig. 6, Supplementary Fig. 7). Figure 6 compares the distribution of the warning-safe response contrast ($\Delta nFR_{(W\text{-}S)}$) recorded in the four different cortical regions studied. Consistent with all previous average population findings, response differences reflecting behavioral meaning of the GO/NO-GO stimuli increase with training and with active performance.

Responses to TORC stimuli depend on both sensory and behavioral context. Encoding of stimulus meaning in VPr and other cortical fields is also demonstrated by the changes in response to the class of TORC stimuli (the set of 30 modulated noise sounds), which had at least three distinct behavioral meanings for the ferrets, depending on context: (1) TORCs served as 'safe' stimuli in the PT-D task (Fig. 1a). We note that the same sequence of stimuli in the PT-D task was played during passive listening but no task—see context (3), and in active task conditions; (2) TORCs were also behaviorally 'neutral anticipatory' stimuli preceding both warning and safe click-trains in the CLR-D task. In this context, TORCs carried virtually no information about the upcoming click rate, but they provided information about the onset time of the upcoming click-train (Fig. 1a). As noted earlier, the same sequence of stimuli in the CLR-D task was played during both passive listening and active task conditions. (3) 'Behaviorally irrelevant' TORCs were also regularly employed to measure STRFs, devoid of any other stimulus task sequence or behavioral task context. Likewise, TORCs

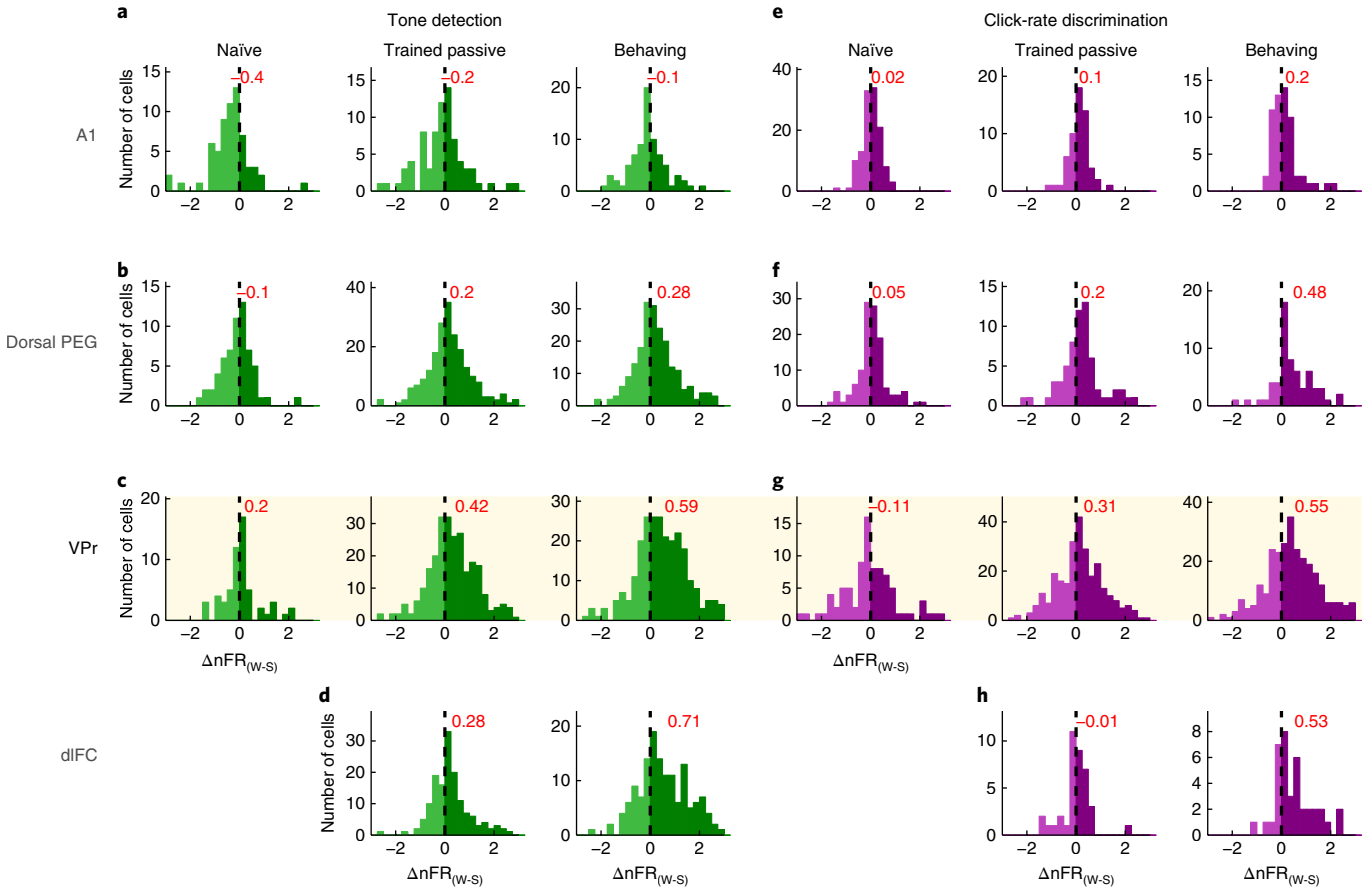

Fig. 6 | Distributions of warning–safe response contrast ($\Delta nFR_{(W-S)}$) data recorded from A1, dorsal PEG, VPr, and dlFC neurons. a–d, Results are shown for the PT-D tasks in naïve and trained animals (in both passive and active conditions). **e–h**, Results are shown for the CLR-D tasks in naïve and trained animals (in both passive and active conditions). $\Delta nFR_{(W-S)}$ was computed as the difference of the mean firing rates (normalized to population maximum) of warning and safe sound responses 0.1–0.45 s after sound onset (PT-D) or 0.3–1.0 s after TORC offset/click onset (CLR-D). The histograms are arranged in three columns for each task, showing contrast in naïve (left column) and trained animals during passive listening (middle column) and during active behavior (right column). The cream shaded area indicates data obtained from VPr. Histograms are mostly symmetric in the naïve animal in all cortical regions recorded. However, in trained animals, a slight asymmetry toward $\Delta nFR_{(W-S)}$ contrast enhancement shows up in the passive state (middle columns), which is further shifted during behavior (right columns). The distributions become progressively more asymmetric in higher cortical areas. Red values display the mean $\Delta nFR_{(W-S)}$. Naïve PT-D: A1, $n=64$; dorsal PEG, $n=61$; VPr, $n=60$ neurons. Trained PT-D: A1, $n=71$; dorsal PEG, $n=199$; VPr, $n=251$; dlFC $n=138$ neurons. Naïve CLR-D: A1, $n=65$; dorsal PEG, $n=60$; VPr, $n=50$ neurons. Trained CLR-D: A1, $n=57$; dorsal PEG, $n=60$; VPr, $n=266$; dlFC $n=38$ neurons.

in the passive presentation PT-D and CLR-D stimuli also played a mostly 'behaviorally irrelevant' role (although the context of the stimulus sequence intermixed with warning sounds might trigger behavioral associations, even in the absence of reward). Therefore, we compared the responses to TORCs in these three contexts in the same cells, and across different cortical regions, to highlight the extent and manner in which responses are shaped both by stimulus context and behavioral meaning (Supplementary Fig. 8). Passive TORC responses were stable across stimulus contexts in A1 and dorsal PEG, but varied between contexts in VPr, differences that were amplified during active engagement in PT-D versus CLR-D tasks (Fig. 5).

Poststimulus persistence of target responses. In addition to exhibiting a large contrast enhancement between warning and safe sounds during the duration of task stimuli, higher cortical areas (especially VPr and dlFC) also showed a persistent response to the warning stimulus after the sound ended. This extended poststimulus response preserved a short-term (800 ms) 'memory' of the contrast after the offset of the warning stimulus, which persisted through the 400 ms pre-shock and 400 ms shock windows (during which the animal had to refrain from licking to avoid shock—see Fig. 1a). This poststimulus activity is also evident in Fig. 3b,c,e,f and in Fig. 4, where the response to the warning stimulus clearly persists in the poststimulus interval. To quantify this post-warning activity, we measured the poststimulus firing rate change from passive to active state in the silent 50–700 ms interval after target offset (Fig. 7 and Supplementary Fig. 9). Post-warning-stimulus response persistence was not observed in A1 and is most apparent in the VPr and dlFC regions. The four cortical areas, A1 (PT-D, $n=71$; CLR-D, $n=57$ neurons), dorsal PEG (PT-D, $n=199$; CLR-D, $n=60$ neurons), VPr (PT-D, $n=251$; CLR-D, $n=266$ neurons), and dlFC (PT-D, $n=138$; CLR-D, $n=38$ neurons) had significantly different poststimulus warning responses in both tasks (Kruskal–Wallis test, PT-D: $\chi^2=40.947$, $P=6.7\times10^{-9}$, d.f. = 3; CLR-D: $\chi^2=12.7391$, $P=0.0052$, d.f. = 3). A post hoc Tukey's HSD test revealed significant differences between higher-order areas (VPr, dlFC) and A1 in the CLR-D task (A1/VPr: effect size ($mean_{(A1)}-mean_{(VPr)}$) = −60.709, 95% CI = (−109.27, −12.14), $P=0.0072$; A1/dlFC: effect size = −70.39, 95% CI = (−139.36, −1.43), $P=0.0433$) and with both

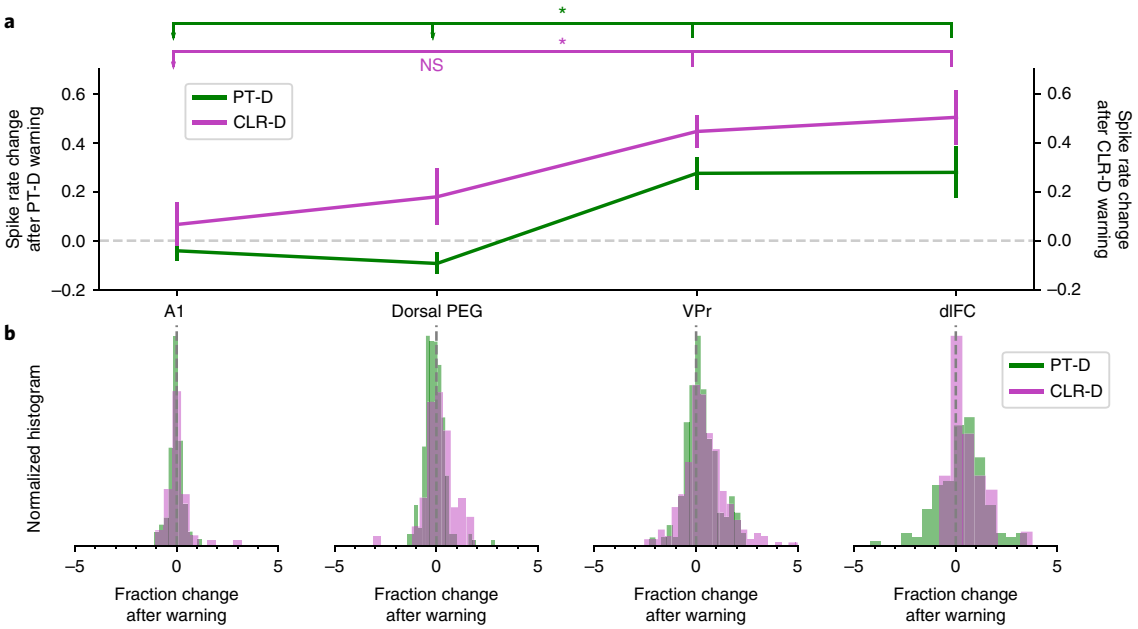

Fig. 7 | VPr and dlFC neurons display a substantial and sustained response during the silent period following warning sound presentation during task performance. This sustained response occurs during a silent period of 800 ms after warning sound offset and lasts until the end of the 400 ms shock time window (see Figs. 1, 3, and 4). We measured this response as the change in normalized mean firing rate from the passive to the behaving state in a time window between 50 and 700 ms after warning sound offset. **a**, Behavior-dependent change in normalized after-warning responses in A1 (PT-D, $n=71$; CLR-D, $n=57$ neurons), dorsal PEG (PT-D, $n=199$; CLR-D, $n=60$ neurons), VPr (PT-D, $n=251$; CLR-D, $n=266$ neurons), and dlFC (PT-D, $n=138$; CLR-D, $n=38$ neurons) in PT-D (green) and CLR-D (purple) tasks (mean ± s.e.m.). In both tasks, VPr and dlFC display a significant increase in their responses after warning sound offset during this silent 650-ms time window (PT-D: $\chi^2=13.4$, $P=0.0052$, d.f. = 3; CLR-D: $\chi^2=40.947$, $P=6.7\times10^{-9}$, d.f. = 3; Kruskal–Wallis test). The asterisks and lines above the curves show Tukey's HSD post hoc pair-wise difference significance between higher-order areas VPr and dlFC with A1 and dorsal PEG (PT-D: A1/VPr , $P=0.0072$; dorsal PEG/VPr, $P=0$; A1/dlFC, $P=0.008$; dorsal PEG/dlFC, $P=0$; CLR-D: A1/VPr, $P=0.0072$; dorsal PEG/VPr, $P=0.3336$; A1/dlFC, $P=0.0433$; dorsal PEG/dlFC, $P=0.4292$). **b**, Normalized distributions of the behavior-dependent change in response after warning sounds in A1, dorsal PEG, VPr and dlFC.

earlier auditory areas (A1, dorsal PEG) in the PT-D task (A1/VPr: effect size = −76.51, 95% CI = (−143.97, −9.06), $P=0.0187$; A1/dlFC: effect size = −90.73, 95% CI = (−164.04, −17.42), $P=0.008$; dorsal PEG/VPr: effect size = −99.33, 95% CI = (−147.42, −51.25), $P=0$; dorsal PEG/dlFC: effect size = −113.55, 95% CI = (−169.54, −57.55), $P=0$). No significant difference was found between VPr and dlFC poststimulus activity in either task (PT-D: effect size = −14.21, 95% CI = (−67.64, 39.21), $P=0.9035$; CLR-D: effect size = −9.69, 95% CI = (−65.74, 46.367), $P=0.9708$).

Discussion

The present results extend our understanding of neural encoding of sound in a higher 'tertiary' auditory cortical region and comprise the first extensive description of neurophysiological responses to acoustic stimuli in the VPr area of the ferret auditory cortex. The findings reveal a profound transformation of responses between passive listening and active behavioral context, producing a representation that is consistent with the emergent behavioral control signals observed in the frontal cortex during the same behaviors. In the quiescent state, VPr responses are distinguishable from those of lower auditory cortical areas (A1, AAF, PPF, PSF) by their significantly longer response latencies, poor phase locking, and broader frequency tuning (Fig. 2). However, the distinctiveness of VPr responses emerges more vividly during active task performance with (1) selective response enhancements to warning stimuli, (2) the unveiling of the long-term effects of learning, and (3) encoding of behavioral meaning of task stimuli not only during a sound, but also after it, reflecting reward contingencies and task-action timing, maintained in short-term memory during behavior. These three characteristic features of VPr responses are discussed in more detail in the next sections.

Enhanced warning sound responses during behavior. Although VPr exhibits task-related plasticity in receptive field and response properties, as demonstrated previously in A1 and dorsal PEG[11,15,17], the greater magnitude, scale, and nature of the current neuroplasticity results place VPr at a higher level in the auditory cortical network, at an intermediate level between dorsal PEG fields (PPF and PSF) and dlFC. This position in the auditory cortical pathway is supported by our neurophysiological findings and also by neuroanatomy. The dramatic selective enhancement of VPr responses to warning sounds during behavior are presumably mediated by the development of new context-dependent neural circuitry during task learning (Fig. 4), which in turn also transforms responses to other task-relevant stimuli depending on behavioral context (Fig. 5, and Supplementary Figs. 2 and 3). A remarkable feature of many VPr cells is how quickly they can transition from general auditory responses (in pre-passive conditions) to highly specific responses to warning sounds (Fig. 3a,c and Supplementary Figs. 2 and 3). Some VPr cells are even more extreme, exhibiting 'frontal-cortex-like' properties[18] in that they show very little or no response to safe or warning sounds in the passive condition, while selectively responding to warning stimuli during active behavior (Supplementary Fig. 3). These results illustrate the importance of behavioral state, as well as stimulus choice, in shaping sustained responses[29]. Although the neural mechanisms for such swift attention-driven transformations are currently unknown, similar rapid changes in response properties have been postulated to reflect top-down influences that dynamically switch local network properties associated with each learned task[30,31]. The top-down effects of task engagement on receptive field plasticity have been shown to reach A1[15] and subcortically even to the inferior colliculus[32]. Although not evident in the population

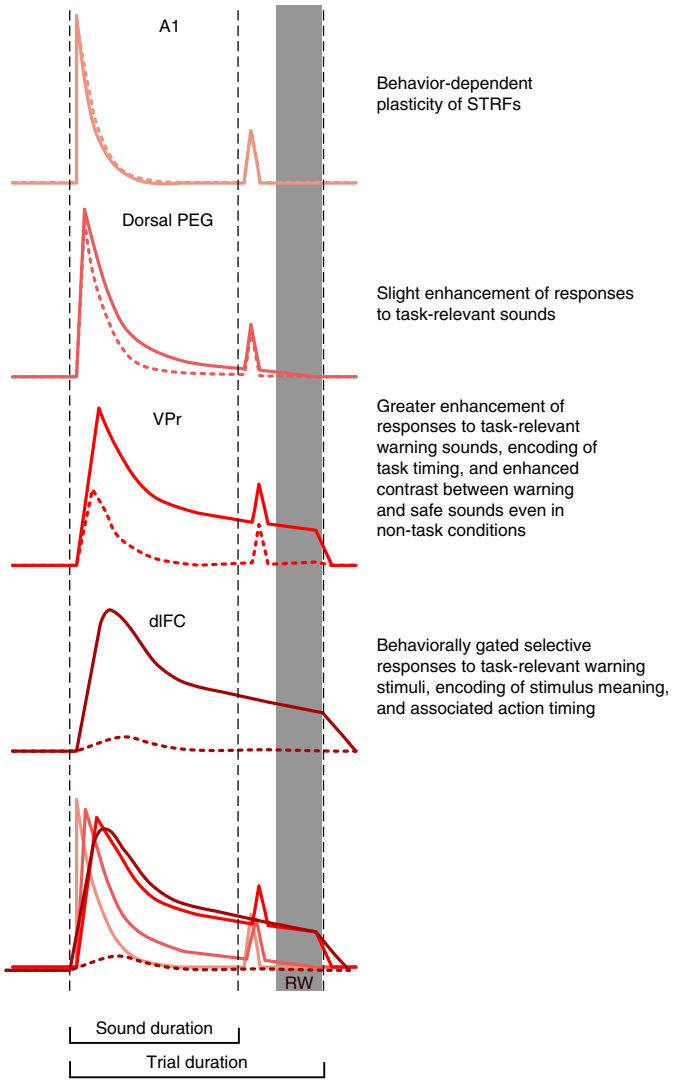

Fig. 8 | Summary of progression of task-related population responses to the warning stimulus along the auditory processing hierarchy in the PT-D task. The overall population-averaged passive response to sound in A1 is slightly suppressed during behavior, particularly for safe stimuli, though less so for warning stimuli. However, in contrast, the responses to warning stimuli are somewhat enhanced in dorsal PEG during behavior, and the responses to warning sounds are even more greatly enhanced in VPr during the active, attentive behavioral state. In the PT-D task, the higher-order auditory cortex (VPr) shares common response properties to warning stimuli with the dlFC, suggesting that the emergence of coding for non-acoustical task features, such as timing and sound meaning, may originate in the higher auditory cortex.

responses recorded in A1 (Figs. 4 and 7, and Supplementary Fig. 9) a recent decoding analysis suggests that poststimulus A1 activity maintains a memory of stimulus behavioral meaning during task engagement[33]. It is possible that this information in A1 is dependent on top-down projections from VPr, dlFC, or other higher areas in the auditory attention network.

Choice probability in VPr. Multiple groups have reported significant choice probability in the auditory cortex, indicating that even sensory neurons carry information about an upcoming decision. Significant choice probability has been found in A1 for one type of auditory task[34], whereas in other tasks, choice probability was only observed in higher auditory cortical areas[10,12]. One recent paper[12] highlighted the causal role of the auditory belt anterior-lateral field in the monkey in contributing to perceptual decision-making. In light of the present results in VPr, we predicted that VPr would be involved in extracting the behavioral meaning of the acoustic stimulus and forming auditory perceptual decisions. However, our analysis of choice probability for the two tasks in the present study did not yield significant results in A1 nor in higher auditory areas as might be predicted from earlier work[12]. However, it is quite possible that different auditory cortical regions play different roles depending on species, task design, level of difficulty, and context. Further studies are needed to test choice probability in VPr in positive reinforcement GO/NO-GO or two-alternative forced choice behavioral paradigms.

Long-term effects of learning in VPr. VPr population responses exhibited a systematic and clear contrast between responses to warning and safe stimuli even in the passive state, but only in trained rather than task-naïve animals (Figs. 5 and 6). This training-dependent enhanced contrast was weak or absent in lower auditory cortical areas (Fig. 5). We ascribe this to the long-term effects of learning that reshape responses in higher cortical areas, such as VPr, based on their behavioral significance. However, in the dlFC these training effects are only evident during behavior because of the absence of any significant responses in the passive state, reflecting behavioral gating[18]. We conjecture that these VPr learning effects may be similar to the experience-dependent malleability of the 'protocortex' described in the visual area inferotemporal cortex after extended training[4].

Sustained poststimulus responses may track reward and motor timing. VPr responses exhibit another dimension that reveals a similarity with dlFC: sustained post-warning responses (Figs. 3 and 4) coding for task timing and the behavioral response window in passive listening, but even more clearly during active task performance. In the two GO/NO-GO conditioned avoidance tasks in the present study[15] animals learned to cease licking during a 400–800 ms window following warning stimulus offset. Activity in the VPr clearly encodes this timing in the form of poststimulus responses that, across different single neurons, (1) occur precisely during this narrow temporal window, (2) persist precisely from stimulus offset up to this window, or (3) persist the full 800 ms and beyond (Fig. 3a,c, and Supplementary Figs. 2, 3, and 9). These poststimulus responses are not present in A1 and begin to appear only in higher auditory areas for both PT-D and CLR-D tasks in VPr and dlFC, as shown in the diagram representation of population-level profiles of passive and active responses in the cortical hierarchy shown in Fig. 8.

This encoding of non-acoustic information, such as task decision, motor response or timing, reward, and task-correlated visual or somatosensory signals is in general accord with earlier findings[34–36] that have emphasized the 'semantic' processing that occurs in the auditory cortex[37].

Evidence for VPr as a tertiary region in the ferret auditory cortex. Neuroanatomical and neurophysiological studies of the ferret auditory cortex over the past three decades (Fig. 1) have revealed the presence of multiple auditory areas, including primary areas such as the A1 and AAF, adjacent secondary areas, such as the ADF, PPF, and PSF, and still higher auditory areas such as the AVF, the anterior and posterior pseudosylvian sulcal cortex (PSSC), and VP[19,20,23,38]. The most recent neuroanatomical connectional data[20] support the idea that in the PEG, PPF and PSF may both be secondary or belt areas, since they reciprocally interconnect with core areas such as the A1 and AAF. In contrast, while there are reciprocal projections from both the PPF and PSF to VP, there do not appear to be projections from core areas to VP[20], suggesting that VP may correspond in hierarchical position to a parabelt auditory area in primates.

VPr can be reliably accessed by carefully mapping tonotopic organization in the medial ectosylvian gyrus (MEG) and PEG,

and determining the position of A1 and PPF, which have mirror tonotopic maps (Fig. 1). In recordings lateral to the high frequency (anterolateral) region of the PPF, there is a sudden and abrupt change in passive response properties and frequency tuning as summarized in Fig. 2, marking the entry into the VPr region. We recorded in the rostral area of VP in an area up to 2–3 mm lateral to the boundary with the PPF, and rostrally up to the PSS. These findings are consistent with the only previously published data on tuning in VP[20,23]. Although future studies will be needed to determine what differences may exist in the responses of the various VP subfields that have been identified[21] (VPr, VP caudal (VPc) and VP ventral (VPv)), as well as their multisensory character and spatial tuning[20], our current VPr results reveal many of the passive auditory response properties associated with an auditory 'parabelt' area, including broader receptive fields, longer latency and duration responses, low SNR, and sparseness. In addition, VPr displays an impressive array of strong behavioral effects, including rapid short-term (driven by attentive task engagement) and long-term task-related plasticity and learning.

Comparison of VPr with the primate parabelt and other tertiary cortical areas. The tertiary sensory cortex is a higher-order cortical sensory area at least two synapses up the cortical hierarchy from primary sensory regions. In the monkey auditory system, the primary (core) regions project to multiple, adjacent areas within a secondary (belt) region, which in turn project to areas in a tertiary (parabelt) region[39,40]. Although the neuroanatomy and connections of parabelt and other regions of the primate auditory cortex have been well elucidated[39–42], and there is an abundance of insight about processing in lower auditory cortical areas from neurophysiological studies of responses in the core and belt, to our knowledge there are only two published studies on the neurophysiological response properties of the parabelt in awake but non-behaving macaque monkeys and marmosets[43,44]. Both studies demonstrate that tone response latencies increase from A1 to belt to parabelt and were longest in the rostral parabelt, which is consistent with our results in the ferret (see Figs. 1f and 2a,d). Similar to primates, belt regions (PPF and PSF) in the ferret receive strong inputs from primary regions (A1 and AAF); in turn, VP receives inputs from the belt regions with no (or negligible) A1 or AAF inputs. Our neurophysiological results are also generally consistent with the possibility that the auditory cortical hierarchy, as in the somatosensory and visual systems, not only follows a hierarchical ordering of increasing response latencies but also of increasingly long temporal windows for sensory integration[45]. Hence, using these criteria of response latency and cortical connectivity, ferret VP is a tertiary region that bears similar features to the parabelt as defined in the primate auditory cortex. Despite these parallels, establishing clear homologies between cortical areas across species is difficult and daunting, especially in higher-order sensory areas[46].To elucidate the relationship between the organization and architecture of auditory cortical areas in carnivores (ferret and cat) and primates, further careful comparative neuroanatomical and neurophysiological studies are required. These future studies are necessary to clarify possible homologies between the ferret dorsal PEG and VPr, the multiple higher auditory cortical regions in the cat[47], and the belt and parabelt regions in the primate auditory cortex.

However, in general, compared to primary sensory regions, secondary and tertiary cortical sensory areas integrate inputs over longer periods of time, show greater context-dependent adaptive plasticity, are more concerned with the associative functions involved in perception, object recognition, and object memory, and have also been shown to be closely linked to perceptual decision-making and action. A recent study of the human tertiary auditory cortex described responses that transform from acoustic to perceptual dimensions in the context of the McGurk effect[48], which illustrates this transformational process in human auditory processing. A comparable tertiary region in the primate visual system may be the inferotemporal cortex, which also plays a key role in object perception and recognition[3,46] as part of the gradual progression from sensory to task-related processing in the cerebral cortex[49].

VPr in the auditory attention cortical network. In conclusion, the physiological response properties of VPr identify a higher field in the ferret auditory cortex, distinct from previously characterized areas, which is situated midway along the auditory cortical network from A1 to dlFC. Responses in the VPr are dynamically driven by selective attention during task engagement and markedly reshaped by task conditions and behavioral state (Figs. 4 and 8). The VPr is also distinctive in showing long-term changes in representation of learned task-relevant stimuli (Fig. 5). Another feature of the VPr is the prominent poststimulus response to warning stimuli that probably reflects an emergent representation of non-acoustic task-related information, such as reward and task timing for action (Figs. 3, 4, 5, and 8, and Supplementary Figs. 2–7). This marks a transition from a nearly veridical acoustic spectrotemporal representation in A1 to a more cognitive representation based on the behavioral meaning associated with incoming sounds in secondary auditory cortical areas (in the dorsal PEG)[11] and even more strongly in tertiary areas such as the VPr. The beginnings of this transition occur as early as A1[15–17,33–37] and even in the inferior colliculus[32], but are most clearly visible in higher auditory cortical areas, such as the VPr, and are influenced by task engagement[10,12,34]. Our results provide new insights into the transformation from sound to behavioral meaning in the auditory pathway[50] and raise new questions as to the neural basis for the differences in task-driven attentional modulation at multiple hierarchical levels of the auditory system, the functional role of the VPr in selective auditory attention and task representation, the mechanisms underlying long-term auditory learning, and the role of top-down projections in mediating higher-level auditory processing.

Online content

Any methods, additional references, Nature Research reporting summaries, source data, statements of data availability and associated accession codes are available at https://doi.org/10.1038/s41593-018-0317-8.

Received: 1 February 2018; Accepted: 5 December 2018;
Published online: 28 January 2019

References

1. Afraz, A., Yamins, D. L. K. & DiCarlo, J. J. Neural mechanisms underlying visual object recognition. *Cold Spring Harb. Symp. Quant. Biol.* **79**, 99–107 (2014).
2. Yau, J. M., Kim, S. S., Thakur, P. H. & Bensmaia, S. J. Feeling form: the neural basis of haptic shape perception. *J. Neurophysiol.* **115**, 631–642 (2016).
3. Kornblith, S. & Tsao, D. Y. How thoughts arise from sights: inferotemporal and prefrontal contributions to vision. *Curr. Opin. Neurobiol.* **46**, 208–218 (2017).
4. Arcaro, M. J., Schade, P. F., Vincent, J. L., Ponce, C. R. & Livingstone, M. S. Seeing faces is necessary for face-domain formation. *Nat. Neurosci.* **20**, 1404–1412 (2017).
5. Hernández-Pérez, R. et al. Tactile object categories can be decoded from the parietal and lateral-occipital cortices. *Neuroscience* **352**, 226–235 (2017).
6. Rossi-Pool, R. et al. Emergence of an abstract categorical code enabling the discrimination of temporally structured tactile stimuli. *Proc. Natl Acad. Sci. USA* **113**, E7966–E7975 (2016).
7. Romo, R., Lemus, L. & de Lafuente, V. Sense, memory, and decision-making in the somatosensory cortical network. *Curr. Opin. Neurobiol.* **22**, 914–919 (2012).
8. Freedman, D. J. & Assad, J. A. Neuronal mechanisms of visual categorization: an abstract view on decision making. *Annu. Rev. Neurosci.* **39**, 129–147 (2016).
9. Rojas-Hortelano, E., Concha, L. & de Lafuente, V. The parietal cortices participate in encoding, short-term memory, and decision-making related to tactile shape. *J. Neurophysiol.* **112**, 1894–1902 (2014).

10. Niwa, M., Johnson, J. S., O'Connor, K. N. & Sutter, M. L. Differences between primary auditory cortex and auditory belt related to encoding and choice for AM sounds. *J. Neurosci.* **33**, 8378–8395 (2013).
11. Atiani, S. et al. Emergent selectivity for task-relevant stimuli in higher-order auditory cortex. *Neuron* **82**, 486–499 (2014).
12. Tsunada, J., Liu, A. S. K., Gold, J. I. & Cohen, Y. E. Causal contribution of primate auditory cortex to auditory perceptual decision-making. *Nat. Neurosci.* **19**, 135–142 (2016).
13. Dong, C., Qin, L., Zhao, Z., Zhong, R. & Sato, Y. Behavioral modulation of neural encoding of click-trains in the primary and nonprimary auditory cortex of cats. *J. Neurosci.* **33**, 13126–13137 (2013).
14. Nodal, F. R. & King, A. J. *Biology and Diseases of the Ferret.* (Wiley-Blackwell, Hoboken, 2014).
15. Fritz, J., Shamma, S., Elhilali, M. & Klein, D. Rapid task-related plasticity of spectrotemporal receptive fields in primary auditory cortex. *Nat. Neurosci.* **6**, 1216–1223 (2003).
16. Fritz, J. B., Elhilali, M. & Shamma, S. A. Differential dynamic plasticity of A1 receptive fields during multiple spectral tasks. *J. Neurosci.* **25**, 7623–7635 (2005).
17. David, S. V., Fritz, J. B. & Shamma, S. A. Task reward structure shapes rapid receptive field plasticity in auditory cortex. *Proc. Natl Acad. Sci. USA* **109**, 2144–2149 (2012).
18. Fritz, J. B., David, S. V., Radtke-Schuller, S., Yin, P. & Shamma, S. A. Adaptive, behaviorally gated, persistent encoding of task-relevant auditory information in ferret frontal cortex. *Nat. Neurosci.* **13**, 1011–1019 (2010).
19. Bizley, J. K., Nodal, F. R., Nelken, I. & King, A. J. Functional organization of ferret auditory cortex. *Cereb. Cortex* **15**, 1637–1653 (2005).
20. Bizley, J. K., Bajo, V. M., Nodal, F. R. & King, A. J. Cortico-cortical connectivity within ferret auditory cortex. *J. Comp. Neurol.* **523**, 2187–2210 (2015).
21. Radtke-Schuller, S. *Cyto- and Myeloarchitectural Brain Atlas of the Ferret* (Springer International, Cham, 2018).
22. Pallas, S. L. & Sur, M. Visual projections induced into the auditory pathway of ferrets: II. Corticocortical connections of primary auditory cortex. *J. Comp. Neurol.* **337**, 317–333 (1993).
23. Bajo, V. M., Nodal, F. R., Bizley, J. K., Moore, D. R. & King, A. J. The ferret auditory cortex: descending projections to the inferior colliculus. *Cereb. Cortex* **17**, 475–491 (2007).
24. Recanzone, G. H., Schreiner, C. E. & Merzenich, M. M. Plasticity in the frequency representation of primary auditory cortex following discrimination training in adult owl monkeys. *J. Neurosci.* **13**, 87–103 (1993).
25. Galván, V. V. & Weinberger, N. M. Long-term consolidation and retention of learning-induced tuning plasticity in the auditory cortex of the guinea pig. *Neurobiol. Learn. Mem.* **77**, 78–108 (2002).
26. Reed, A. et al. Cortical map plasticity improves learning but is not necessary for improved performance. *Neuron* **70**, 121–131 (2011).
27. Froemke, R. C. et al. Long-term modification of cortical synapses improves sensory perception. *Nat. Neurosci.* **16**, 79–88 (2013).
28. Bieszczad, K. M., Miasnikov, A. A. & Weinberger, N. M. Remodeling sensory cortical maps implants specific behavioral memory. *Neuroscience* **246**, 40–51 (2013).
29. Wang, X., Lu, T., Snider, R. K. & Liang, L. Sustained firing in auditory cortex evoked by preferred stimuli. *Nature* **435**, 341–346 (2005).
30. Gilbert, C. D. & Li, W. Top-down influences on visual processing. *Nat. Rev. Neurosci.* **14**, 350–363 (2013).
31. Caras, M. L. & Sanes, D. H. Top-down modulation of sensory cortex gates perceptual learning. *Proc. Natl Acad. Sci. USA* **114**, 9972–9977 (2017).
32. Slee, S. J. & David, S. V. Rapid task-related plasticity of spectrotemporal receptive fields in the auditory midbrain. *J. Neurosci.* **35**, 13090–13102 (2015).
33. Bagur, S. et al. Go/no-go task engagement enhances population representation of target stimuli in primary auditory cortex. *Nat. Commun.* **9**, 2529 (2018).
34. Bizley, J. K., Walker, K. M. M., Nodal, F. R., King, A. J. & Schnupp, J. W. H. Auditory cortex represents both pitch judgments and the corresponding acoustic cues. *Curr. Biol.* **23**, 620–625 (2013).
35. Brosch, M., Selezneva, E. & Scheich, H. Nonauditory events of a behavioral procedure activate auditory cortex of highly trained monkeys. *J. Neurosci.* **25**, 6797–6806 (2005).
36. Yin, P., Mishkin, M., Sutter, M. & Fritz, J. B. Early stages of melody processing: stimulus-sequence and task-dependent neuronal activity in monkey auditory cortical fields A1 and R. *J. Neurophysiol.* **100**, 3009–3029 (2008).
37. Scheich, H. et al. Behavioral semantics of learning and crossmodal processing in auditory cortex: the semantic processor concept. *Hear. Res.* **271**, 3–15 (2011).
38. Kelly, J. B., Judge, P. W. & Phillips, D. P. Representation of the cochlea in primary auditory cortex of the ferret (*Mustela putorius*). *Hear. Res.* **24**, 111–115 (1986).
39. Kaas, J. H. & Hackett, T. A. Subdivisions of auditory cortex and processing streams in primates. *Proc. Natl Acad. Sci. USA* **97**, 11793–11799 (2000).
40. Hackett, T. A. Information flow in the auditory cortical network. *Hear. Res.* **271**, 133–146 (2011).
41. Hackett, T. A. et al. Feedforward and feedback projections of caudal belt and parabelt areas of auditory cortex: refining the hierarchical model. *Front. Neurosci.* **8**, 72 (2014).
42. Plakke, B. & Romanski, L. M. Auditory connections and functions of prefrontal cortex. *Front. Neurosci.* **8**, 199 (2014).
43. Camalier, C. R., D'Angelo, W. R., Sterbing-D'Angelo, S. J., de la Mothe, L. A. & Hackett, T. A. Neural latencies across auditory cortex of macaque support a dorsal stream supramodal timing advantage in primates. *Proc. Natl Acad. Sci. USA* **109**, 18168–18173 (2012).
44. Kajikawa, Y. et al. Auditory properties in the parabelt regions of the superior temporal gyrus in the awake macaque monkey: an initial survey. *J. Neurosci.* **35**, 4140–4150 (2015).
45. Murray, J. D. et al. A hierarchy of intrinsic timescales across primate cortex. *Nat. Neurosci.* **17**, 1661–1663 (2014).
46. Kaas, J. H. The future of mapping sensory cortex in primates: three of many remaining issues. *Philos. Trans. R. Soc. Lond. B Biol. Sci.* **360**, 653–664 (2005).
47. Winer, J. A. & Lee, C. C. The distributed auditory cortex. *Hear. Res.* **229**, 3–13 (2007).
48. Smith, E. et al. Seeing is believing: neural representations of visual stimuli in human auditory cortex correlate with illusory auditory perceptions. *PLoS One* **8**, e73148 (2013).
49. Brincat, S. L., Siegel, M., von Nicolai, C. & Miller, E. K. Gradual progression from sensory to task-related processing in cerebral cortex. *Proc. Natl Acad. Sci. USA* **115**, E7202–E7211 (2018).
50. Bizley, J. K. & Cohen, Y. E. The what, where and how of auditory-object perception. *Nat. Rev. Neurosci.* **14**, 693–707 (2013).

Acknowledgements

We thank C. Bimbard, K. Dutta, and N. Joshi for their assistance with the neurophysiological recordings, A. Meredith and K. Dutta for their assistance with the neuroanatomical experiments, and L. Artemisia for support. This research was funded by grants from the US National Institutes of Health (grants R01-DC-005779 to S.A.S. and J.B.F. and R01-DC-014950 to S.V.D.) and by a DARPA grant (N660011724009) to J.B.F. D.D. held an AGAUR fellowship (Generalitat de Catalunya) in the frame of the EU COFUND Marie-Curie program (no. 2014BP-A00226) and an Erasmus Mundus ACN fellowship. D.E. held scholarships from CONICYT-PCHA/BECAS CHILE, Doctorado Convocatoria 2009-folio 72100839, Postdoctorado/Convocatoria 2016-folio 74170109, and Fulbright-Institute of International Education.

Author contributions

J.B.F., D.E., and S.A.S. designed the experiments. D.E., P.Y., D.D., and J.B.F. performed the experiments. D.E., S.V.D., and P.Y. analyzed the physiological results. S.R-S. analyzed the neuroanatomical results. D.E. prepared the physiological figures. S.R-S. and D.E. prepared the neuroanatomical figures. J.B.F., D.E., S.V.D., and S.A.S. wrote the manuscript.

Competing interests

The authors declare no competing interests.

Additional information

Supplementary information is available for this paper at https://doi.org/10.1038/s41593-018-0317-8.

Reprints and permissions information is available at www.nature.com/reprints.

Correspondence and requests for materials should be addressed to J.B.F.

Publisher's note: Springer Nature remains neutral with regard to jurisdictional claims in published maps and institutional affiliations.

© The Author(s), under exclusive licence to Springer Nature America, Inc. 2019

Methods

Training and behavioral tasks. We measured the auditory response properties of cortical single units in the auditory and frontal cortices of awake animals during passive listening to experimental sounds and during performance of auditory tasks. All animals used were female, de-scented, neutered, 1–4-year-old adult ferrets (*Mustela putorius furo*) obtained from Marshall BioResources. Three additional untrained (task-naïve) ferrets were used to map the auditory areas and for the anatomical studies, one of which was also used for naïve passive recordings (Figs. 5 and 6). To compare the VPr data with other auditory cortical areas, such as the A1, dorsal PEG, dlFC, we also reanalyzed data from 14 animals that were trained and recorded for previous behavior studies of the A1, dorsal PEG, and dlFC[11,15,17,18], and from a total of 32 (including responses from 18 additional animals used in previously published studies from our laboratory) to compare the VPr tuning properties with the A1 and dorsal PEG during passive listening (Fig. 2). Animals were randomly chosen from the colony for experimentation. Some animals were directly implanted with headposts for naïve neurophysiological recordings. Other animals were trained on auditory tasks and were implanted with headposts and used for behavioral neurophysiological recordings. All experimental procedures were approved by the University of Maryland Animal Care and Use Committee and conformed to the standards specified by the National Institutes of Health.

We trained four animals on two auditory discrimination tasks with a conditioned avoidance paradigm:[51] PT-D[11,15,17,18] and CLR-D. In both tasks, animals were presented with a series of 1–6 reference 'safe' sounds on each behavioral trial, followed by a target 'warning' sound. No warning sounds were presented on catch trials. Ferrets learned to freely lick water flowing continuously from a spout during presentation of safe sounds, and to briefly refrain from licking after the warning stimulus offset (for a minimum of 400 ms in a 400–800 ms poststimulus window) to avoid receiving a mild tail shock. In the PT-D task, safe sounds consisted of 1–2 s duration broadband rippled noise (TORCs[52]), and warning sounds were pure tones (duration and sound level matched to the TORC references) of equal amplitude. In the CLR-D task, both safe and warning sounds were composed of 1.25 s TORCs immediately followed by a 0.75 s click-train, but the warning click rate was fixed to be either higher or lower than the safe click-train. The click-train rates used in CLR-D varied from 4 to 48 Hz and animals ($n=4$) were trained in one of the two directions of the task, meaning that half of the ferrets ($n=2/4$) were trained with low-rate safe click-trains (4–24 Hz) and high-rate warning click-trains (16–48 Hz), while the other half ($n=2/4$) were trained with high-rate safe click-trains and low-rate warning click-trains. The distribution of click rates used is shown in Supplementary Fig. 4 (panel A). The minimum rate difference between the safe and warning click-trains was 7 Hz, while the maximum was 32 Hz. The distribution of high-to-low click rate ratios used in every behavioral block is shown in Supplementary Fig. 4 (panel B). The mean ($\pm$s.d.) ratio used was 3.2 ± 1.09. All animals trained in the click-rate discrimination task were also trained in the tone detection task ($n=4$) and recordings were made from all four cortical areas—A1, dorsal PEG, VPr, and dlFC. However, the animals from earlier published studies (recordings in A1, dorsal PEG, and dlFC but not in VPr) were exclusively trained on the tone detection task ($n=14$).

The warning sound frequency in the tone detection task, and safe and warning click-train rates in the click discrimination task, were varied among the experiments and training sessions, but were held fixed during a single behavioral block. This variability across training days lead the animals to generalize their behavioral responses to any warning tone frequency or warning click-train rate. Warning tone frequency was chosen after assessing the frequency tuning of the neurons at hand by presenting tone pips (100 ms) of random frequencies (125–32,000 Hz). We chose warning frequencies that evoked the strongest possible responses in all neurons being recorded. Similarly, click rates for safe and warning sounds were chosen after presenting click-trains 4–60 Hz. Sometimes, the broad frequency and click-rate tuning of VPr neurons did not allow to choose a best frequency or click rate; in those cases, we chose a frequency or click rate that evoked responses for most neurons being recorded. The sound level (65–70 dB sound pressure level (SPL)), sound durations (1 or 2 s in tone detection, 2 s in click-rate discrimination), and interstimulus intervals (1.2 or 1.6 s) were kept fixed in a single training or recording session as well. During electrophysiological recording sessions, the task stimulus set was presented before (pre-passive) and after (post-passive) behavior, while the animal passively listened to task sounds and no water was provided (that is, the animal did not engage in the task and displayed no licking behavior). The normal duration of a behavioral block was 10–15 min, which depended on the duration of task sounds and on how thirsty animals were at a given time (each trial was initiated only after a lick); in cases were animals were not very thirsty and licked less frequently, the behavioral block duration could extend up to 20 min. Passive task blocks were usually 7–12 min long, depending on the duration of task sounds.

No blinding was used in the study; this is common in behavioral neuroscience. However, all analyses of neural responses were conducted in the same way for all data acquired over a period of ~15 years in our laboratory, including data from multiple animals and investigators. The neuroanatomical studies were conducted by a researcher who was not directly involved in the behavioral or neurophysiological studies, received brains to process, and during histological processing was blind to each animal history.

Surgery. Initially, animals were trained in a freely moving setting until they reached a consistent and acceptable performance, that is, achieving > 80% hit rate accuracy and <20% false alarm rate for a discrimination rate > 0.65 in at least two consecutive training sessions[15,18]. To secure stable electrophysiological recordings, ferrets were surgically implanted with a stainless steel headpost that was attached to the sagittal interparietal suture. During surgery, ferrets were anesthetized with a combination of ketamine (35 mg kg^{-1} intramuscularly) and dexmedetomidine (0.03 mg kg^{-1} subcutaneously) for induction; deep levels of anesthesia were maintained with 1–2% isoflurane throughout the surgery. Animals were also medicated with atropine sulfate (0.05 mg kg^{-1} subcutaneously) to control salivation and to increase heart and respiratory rates. During surgery, electrocardiogram, pulse, and blood oxygenation were monitored, and rectal temperature was maintained at ~38 °C. Using a sterile procedure, and to be able to reach the ventral areas of the auditory cortex, the skull was surgically exposed by making a midline incision in the scalp and by dissecting both temporal muscles from their insertion in the sagittal interparietal crest down to the level of the zygomatic arch. The headpost was secured in the skull with titanium screws and polycarboxylate cement; then, areas surrounding the frontal and auditory cortices were covered with bone cement (Zimmer Biomet), leaving small (2–3 mm^2) cavities for easy access to the auditory and frontal cortex in both hemispheres. Following surgery, antibiotics (cefazolin, 25 mg kg^{-1}subcutaneously) and analgesics (dexamethasone 2 mg kg^{-1} subcutaneously and flunixin meglumine 0.3 mg kg^{-1} subcutaneously) were administered.

Animals were allowed to recover for ~2 weeks before being habituated to a head restraint in a customized Lucite horizontal cylindrical holder for a period of 1–2 weeks, and then retrained to criterion on the tasks for an additional 2–3 weeks while restrained in the holder. Before the recording sessions, small craniotomies were made over the auditory or frontal cortex and, in simultaneous recording experiments, the ipsilateral auditory and frontal cortices. The bone cement implant securing the headpost, and the sterile impression material placed in the wells between recording sessions, allowed the craniotomies to be kept well protected from the environment. The wells in the head cap implant containing the craniotomies were kept sealed between experiments with sterile vinyl polysiloxane impression material (EXAMIX NDS; GC America, Inc.) and were cleaned and treated with topical antiseptic drugs (povidone-iodine) and antibiotics (cefazolin or enrofloxacin, 0.2 ml) at least once per week. The skin surrounding the implant was cleaned three times per week with warm saline and treated with povidone-iodine and sulfadiazine cream ointment.

Neurophysiological recordings. Training and neurophysiological recording experiments were conducted in a double-walled sound-attenuating chamber (IAC). High impedance (2–6 MΩ at 1 kHz) tungsten microelectrodes (FHC) were used for extracellular neurophysiological recordings and stainless steel electrodes (FHC or Microprobes) for iron deposit markings. Electrodes were arranged in a four-electrode square array and separated by 0.5 mm from their nearest neighbor. In each recording session, four electrodes per recording area (four in the auditory and four in the frontal cortex) were independently advanced through the dura into the cerebral cortex using an EPS drive system (Alpha-Omega). Electrodes were slowly and independently advanced until good spike isolation was found in the majority of the electrodes. Data acquisition was performed with an AlphaLab data acquisition system (Alpha-Omega), signals recorded at 25,000 samples s^{-1} and amplified 15,000×. Additionally, 18 recording sessions in the primary auditory cortex were performed in a subset of 2 animals using a 24-electrode linear array (Plexon U-Probe) with 75 µm between electrode contacts and impedances between 275 and 1,500 kΩ at 1 kHz, using Plexon and Triangle BioSystems International 1× headstages, amplified with Plexon preamplifiers and acquired using MANTA v. 1.0, an open-source data acquisition suite written for MATLAB[53]. Single units (usually one or two per electrode) were isolated by *k*-means clustering using custom software written in MATLAB or the open-source software Klusta (version c1909dd)[54]. Sound stimuli, behavioral operation, online analysis, and recording triggering were controlled with customized open-source software (Behavioral Auditory PHYsiology (BAPHY)).

Localization of auditory fields and recording sites. Before recording activity in non-primary auditory areas, initial recordings were directed to A1 and determined by the relative distance to external cranial landmarks. In female ferrets, A1 is located approximately 16 mm anterior to the occipital midline crest and 12 mm lateral to the skull midline. During the initial recording sessions in each animal, small craniotomies were placed above A1 using these coordinates; A1 responses were confirmed by analyzing the tuning properties of the recorded cells in response to 100 ms tone pips of random frequencies spanning 8 oct, presented at intervals of 1 s. Also, 3 s TORCs were used to compute STRFs. A1 neurons are known to present sharp tuning to pure tones and clear single-peak, short latency STRFs[11,15,19]. Determination of neuronal best frequencies allowed us to confirm the location of A1 based on its characteristic tonotopic organization of high-to-low frequency gradient in a dorsoventral direction[19]. Then, by ventrally expanding the existing craniotomy it was possible to gain access to non-primary auditory areas in the PEG[19,22]. Two subfields in the dorsal PEG, PPF, and PSF, display a reversal in the tonotopic map, sharing a low frequency area with A1 and displaying higher

frequency regions more ventrally. Both fields are also separated by a low frequency border, meaning that PSF displays a low-to-high frequency tonotopic gradient in an anterodorsal to posteroventral direction, while PPF displays low frequencies posterodorsally and high frequencies anteroventrally[11,19]. Neurons in these areas display broader tuning, longer latencies, and longer sustained responses than A1 (Fig. 2), and their STRFs display more complex patterns of excitatory and inhibitory subfields, with more numerous, longer, and less compact excitatory and inhibitory subfields in both the spectral and temporal axes[11]. The locations of the dorsal PEG recordings were confirmed by checking the tuning properties of its neurons and their location relative to the tonotopic map.

VPr recordings were directed to a region ventral to the high-frequency region of the PPF. VPr spans an area 1–2 mm below and ventral to high-frequency PPF and ventral to the lower lip of the PSS. Partly because of its extreme lateral location and limited accessibility for surface recordings, VP has remained one of the least studied areas of the ferret auditory cortex. Localization of VPr was based on a tonotopic discontinuity at the high end of the frequency map in the adjacent PPF area, which is characterized by a posteromedial-anterolateral tonotopic gradient from low to high frequency tuning[11,19]. The transition from PPF to VPr is characterized by a sharp transition in frequency tuning from high to lower best frequency and often much broader frequency tuning (Fig. 1d,e). VPr also is characterized by much longer onset response latencies (see Fig. 1f). Careful measurements of the location of the recording electrode relative to two reference marks placed in the bone cement surrounding the craniotomy and to a mark at the center of the headpost, were recorded for later reconstruction of electrode penetration sites. The locations of recordings in the VPr (see Supplementary Fig. 1) were marked with electrolytic lesions or iron deposits by passing a small current (10 µA) for 5 min using stainless steel electrodes. Postmortem confirmation of iron deposits was determined by histological examination of Prussian blue reactions.

Stimuli. All acoustical stimuli were presented at 65–70 dB SPL, with the exception of a wider range of amplitudes specifically for the tones (which varied from 40 to 80 dB SPL) used for multilevel tuning assessment and to measure the frequency response curves. Sounds were digitally generated at 40 kHz with custom-made MATLAB functions and A/D hardware (PCI-6052E; National Instruments) and presented with a free-field speaker positioned 30 cm in front of the animal's head. Tones (5 ms onset and offset ramps) were used as target stimuli in the tone detection task and, previous to any behavioral testing, to assess frequency tuning by using tone pips of random frequencies spanning eight octaves. Individual clicks in the click-rate discrimination task (occurring after TORCs in sequential TORC-click-train stimuli; see Fig. 1a) and during passive testing of click tuning with 1 s click-trains of randomly varying click rates from 4 to 60 Hz, were composed of 0.01 s square pulses of alternating polarity. Thirty distinct TORCs were used as task distractor (safe) sounds and also for the computation of STRFs in and out of task context. TORCs were randomly chosen without replacement from a set of 30 TORCs for each TORC set repetition. Each TORC was composed of a 5 oct-wide broadband noise with a dynamic spectrotemporal profile, that is, the superposition of the envelopes of 6 temporally orthogonal ripples (for 4–24 Hz TORCs) or 12 temporally orthogonal ripples (4–48 Hz TORCs). Ripples composing the TORCs had linear sinusoidal spectral profiles, with peaks equally spaced at 0 (flat) to 1.2 cycles per octave; the envelope drifted temporally up or down the logarithmic frequency axis at a constant velocity[52,55]. The envelope of these ripples drifted temporally up or down the logarithmic frequency axis at a constant velocity (4–48 or 4–24 Hz). The 5-oct spectrum of TORCs could be varied in several ranges and was chosen at each recording session to best span the frequencies of the neurons being recorded.

Data analysis. Offline data analyses were performed with custom-made MATLAB and Python scripts. Figures were created using MATLAB (R2010b) functions, Matplotlib (version 3.0.2), Seaborn version 0.9.0 Python libraries, and Inkscape (version 0.92.3). No statistical methods were used to predetermine sample sizes (see Life Sciences Reporting Summary).

Basic tuning properties were determined by analyzing the responses to random frequency tones spanning 6−8 oct (11 tones per octave), usually ranging from 125 Hz to 32 kHz at 65−70 dB SPL. A Gaussian function was fitted to the mean firing rate during a window of 100 ms after tone onset. Best frequency was determined to be the mean of the Gaussian curve; tuning spectral bandwidth was measured as its width in octaves at half-height. Tones presented had a duration of 100 ms and were presented at 1 s intervals. Response latency was measured from the PSTH binned at 1 ms and computed from the responses to all pure frequency tones by measuring the time from tone onset to the peak spike rate in a 100 ms window.

TORCs were also presented to compute STRFs by means of reverse correlation[52] between a time-varying neural response (that is, spikes, multiunit activity) and the spectrogram of the TORCs presented during the experiments. Positive STRF values indicate the time and frequency components of the TORCs correlated with increased neural responses (that is, an excitatory field), whereas negative values indicate components correlated with decreased responses (that is, a suppressive or inhibitory field). The reliability of responses to TORCs, and the quality of the resulting STRFs, was measured by an SNR, computed as the ratio of power in the average PSTH response to all TORCs to power in the difference of single-trial responses from the PSTH[55]. Only responses with SNR values equal or higher than 0.2 were used. Response duration was measured as the width at half-height of the STRF positively rectified and averaged over frequency. STRFs varied in their complexity between auditory areas, with clear excitatory/inhibitory fields in a narrow spectrotemporal range in A1 and more complex tuning in higher-order auditory areas. To compare tuning complexity between areas, we measured an STRF sparseness index, computed as the peak magnitude of the STRF, divided by the s.d. across STRF bins[11]. Higher sparseness values are associated with sharply tuned STRFs concentrated over a few contiguous bins. Consistent with the observation of greater complexity in downstream areas, A1 sparseness index values were greater than for higher-order auditory neurons. Both the Kruskal–Wallis and Tukey's HSD post hoc tests were conducted to examine differences in tuning parameters between areas. We decided to use the Kruskal–Wallis test instead of a one-way ANOVA because all tuning parameter distributions, with the exception of VPr bandwidth ($P=0.268$, Lilliefors test), significantly deviated from normality (Lilliefors test, $P<0.001$).

Single-unit neural responses to task stimuli were measured by computing PSTHs by binning spikes at 30 Hz and obtaining the mean and s.e.m. of the spike rates obtained over all safe and warning sound classes. We only analyzed responses to task sounds from neurons that showed significant responses to auditory stimuli. Units were considered auditory-responsive neurons when there were at least 2 bins (33.3 ms bins) significantly modulated from baseline in the PSTH in response to any (safe or warning) sound ($P<0.05$, jack-knifed t-test, Bonferroni-corrected). The significance of behavioral effects within cells was measured by performing a Wilcoxon signed-rank test, corrected for multiple comparisons using a false discovery rate[56], between the passive and active PSTHs of each sound class (safe or warning). Neural responses were considered to be significantly modulated by behavior (comparing active versus passive responses) if there were at least two consecutive, significant (Wilcoxon signed-rank test, $P<0.05$) PSTH bins within the responses to any task sound class (safe or warning stimuli). Normalized average PSTHs were computed by subtracting the baseline firing rate (measured during the silent pre-stimulus period) from each neuron and then dividing the firing rates of each neuron by the peak modulation of the mean population PSTH, thus adjusting the scale to spikes s^{-1}above or below spontaneous activity. The mean and s.e.m. of each PSTH bin were calculated using a jack-knife procedure[57]. We calculated choice probability from data from all auditory cortical areas in our study using the method described by Niwa et al.[58].

Motor-related lick responses. As in a previous paper[18], we determined significant neural modulation of neuronal activity in the VPr by auditory stimuli using a stepwise linear regression of time-varying spike activity (binned at 50 ms) against stimulus (safe and warning sounds) and motor (licking) events. The complete regression-modeled spiking activity as a function of safe/warning sounds and lick events is shown in equation (1).

$$r(t) = \sum_{\tau=-T}^{T} h_s(\tau)s_s(t-\tau) + h_w(\tau)s_w(t-\tau) + h_m(\tau)m(t-\tau) \quad (1)$$

The stimulus functions, $s_s(t)$ and $s_w(t)$, are 0, except at times, t, of safe or warning sound onset, respectively, when they have a value of 1. Similarly, the motor function, $m(t)$, has a value of 0 except at times when lick events occur. The regression functions, $h_s(\tau)$, $h_w(\tau)$, and $h_m(\tau)$, then indicate the average firing rate before and after each corresponding event. τ is the time lag (in ms) between either (a) stimulus onset or (b) lick event relative to the spike response. Spiking activity is correlated with events at different time lags which can precede (possible predictive spikes) or follow (possible causal spikes) the stimulus onset (sensory) or lick (motor) events. T indicates the range of possible time lags over which the relevant event (stimulus or lick) might correlate with spiking and was set at 500 ms. The regression functions were fitted using normalized reverse correlation, which discounted the spurious effects that might arise as a result of correlations between stimulus events and changes in motor activity. Neurons were classified as being significantly modulated by sensory inputs if the occurrence of a stimulus predicted a change in firing rate that could not be explained by a simpler model on the basis of motor activity alone (equation (2)).

$$r(t) = \sum_{\tau=-T}^{T} h_m(\tau)m(t-\tau) \quad (2)$$

Thus, a neuron was considered to be modulated by sensory inputs only if the full model predicted spiking activity significantly better than the model based only on licking activity ($P<0.05$, jack-knifed t-test).

Statistical analysis. To quantify the differences in target/reference response contrast in passive and active behavior conditions, we used a three-way repeated-measures ANOVA for response differences between warning and safe sounds, with 'area' (A1, dorsal PEG, VPr and dlFC) and 'condition' (passive and behavior) as fixed factors, and 'neuron' nested in 'area' as a random intercept. For the PT-D task, we calculated the response difference (spikes s^{-1}) for each neuron in a time window between 100 ms after stimulus onset (avoiding the purely sensory-driven onset

transient) and the end of the shock period (800 ms poststimulus offset). For the CLR-D task, we calculated the response difference (spikes s^{-1}) for the time window between 300 ms following click-train onset and the end of the shock period (800 ms poststimulus offset). We used Tukey's range test for the post hoc analysis.

Since the VPr and dlFC areas display qualitative differences in their response patterns with the A1 and dorsal PEG areas, we measured responses in two different epochs: (1) during the duration of task-relevant sounds; and (2) in the silent period after presentation of target sounds. We quantified the contrast between safe and warning responses ($\Delta nFR_{(W\text{-}S)}$) in a time window between 0.1 and 0.45 s after sound onset (PT-D task) or 0.3 and 1.0 s (CLR-D task) to avoid onset transient responses and, in the CLR-D task, the offset response to TORCs preceding click-trains. We measured the mean values of $\Delta nFR_{(W\text{-}S)}$ from the normalized PSTH responses to compare population responses between areas and between the trained and naïve animals. The responses observed in the silent period after task target sounds were measured as the change in response from passive to active behavior conditions in a time window of 650 ms starting 50 ms after target offset. Responses recorded during 'miss' trials, when the animal failed to report detection of a warning sound, were discarded to avoid contamination of the data with shock artifacts. Area comparison of poststimulus warning responses was performed with a Kruskal–Wallis test; pairwise area comparisons were performed with Tukey's HSD range test as a post hoc test. The distributions of $\Delta nFR_{(W\text{-}S)}$ data calculated from the A1, dorsal PEG,VPr and dlFC responses in passive and active conditions were tested for normality with a Lilliefors test. All distributions of $\Delta nFR_{(W\text{-}S)}$ were found to significantly deviate from normality ($P<0.05$) with the exceptions of three distributions collected in the CLR-D task context: A1 passive $\Delta nFR_{(W\text{-}S)}$ ($P=0.1586$, $ks=0.1039$); dorsal PEG active $\Delta nFR_{(W\text{-}S)}$ ($P=0.0595$, $ks=0.192$); and dlFC active $\Delta nFR_{(W\text{-}S)}$ ($P=0.1198$, $ks=0.1271$).

Reporting Summary. Further information on research design is available in the Nature Research Reporting Summary linked to this article.

Code availability. The custom scripts written in MATLAB and Python used in this study are available from the corresponding author upon reasonable request.

Data availability

The data supporting the study findings are available from the corresponding author upon reasonable request.

References

51. Heffner, H. E. & Heffner, R. S. in *Methods in Comparative Psychoacoustics* (eds Klump, G. M. et al.) 79–93 (Birkhäuser, Basel, 1995).
52. Klein, D. J., Depireux, D. A., Simon, J. Z. & Shamma, S. A. Robust spectrotemporal reverse correlation for the auditory system: optimizing stimulus design. *J. Comput. Neurosci.* **9**, 85–111 (2000).
53. Englitz, B., David, S. V., Sorenson, M. D. & Shamma, S. A. MANTA—an open-source, high density electrophysiology recording suite for MATLAB. *Front. Neural Circuits* **7**, 69 (2013).
54. Rossant, C. et al. Spike sorting for large, dense electrode arrays. *Nat. Neurosci.* **19**, 634–641 (2016).
55. Depireux, D. A., Simon, J. Z., Klein, D. J. & Shamma, S. A. Spectro-temporal response field characterization with dynamic ripples in ferret primary auditory cortex. *J. Neurophysiol.* **85**, 1220–1234 (2001).
56. Benjamini, Y. & Yekutieli, D. The control of the false discovery rate in multiple testing under dependency. *Ann. Stat.* **29**, 1165–1188 (2001).
57. Efron, B. & Tibshirani, R. *An Introduction to the Bootstrap* (Chapman & Hall, Boca Raton, 1994).
58. Niwa, M., Johnson, J. S., O'Connor, K. N. & Sutter, M. L. Activity related to perceptual judgment and action in primary auditory cortex. *J. Neurosci.* **32**, 3193–3210 (2012).

nature research

Corresponding author(s): Jonathan B. Fritz

Reporting Summary

Nature Research wishes to improve the reproducibility of the work that we publish. This form provides structure for consistency and transparency in reporting. For further information on Nature Research policies, see Authors & Referees and the Editorial Policy Checklist.

Statistical parameters

When statistical analyses are reported, confirm that the following items are present in the relevant location (e.g. figure legend, table legend, main text, or Methods section).

n/a	Confirmed	
☐	☒	The exact sample size (*n*) for each experimental group/condition, given as a discrete number and unit of measurement
☐	☒	An indication of whether measurements were taken from distinct samples or whether the same sample was measured repeatedly
☐	☒	The statistical test(s) used AND whether they are one- or two-sided *Only common tests should be described solely by name; describe more complex techniques in the Methods section.*
☐	☒	A description of all covariates tested
☐	☒	A description of any assumptions or corrections, such as tests of normality and adjustment for multiple comparisons
☐	☒	A full description of the statistics including central tendency (e.g. means) or other basic estimates (e.g. regression coefficient) AND variation (e.g. standard deviation) or associated estimates of uncertainty (e.g. confidence intervals)
☐	☒	For null hypothesis testing, the test statistic (e.g. *F*, *t*, *r*) with confidence intervals, effect sizes, degrees of freedom and *P* value noted *Give P values as exact values whenever suitable.*
☒	☐	For Bayesian analysis, information on the choice of priors and Markov chain Monte Carlo settings
☒	☐	For hierarchical and complex designs, identification of the appropriate level for tests and full reporting of outcomes
☐	☒	Estimates of effect sizes (e.g. Cohen's *d*, Pearson's *r*), indicating how they were calculated
☐	☒	Clearly defined error bars *State explicitly what error bars represent (e.g. SD, SE, CI)*

Our web collection on statistics for biologists may be useful.

Software and code

Policy information about availability of computer code

Data collection	Most data was collected using AlphaMap 10.10 software from AlphaOmega (Nazareth, Israel). Additional data was collected using open-source programs Baphy (commit E155036, https://bitbucket.org/lbhb/baphy) and MANTA 1.0 (https://code.google.com/archive/p/manta-system/), both coded in MATLAB R2010B (from MathWorks, Natick, MA).
Data analysis	Data was analyzed using custom code written in MATLAB R2010B (MathWorks, Natick, MA) and its integrated functions. Figures 5,7 and S9 were prepared with Python 3.7, using the Matplotlib 3.0.2 library and Seaborn 0.9.0. Spike sorting was performed using custom code written in MATLAB R2010B and some data was sorted with open-source program Klusta (version c1909dd, Rossant, C. et al. Spike sorting for large, dense electrode arrays. Nat. Neurosci. 19, 634–641 (2016) doi:10.1038/nn.4268)

For manuscripts utilizing custom algorithms or software that are central to the research but not yet described in published literature, software must be made available to editors/reviewers upon request. We strongly encourage code deposition in a community repository (e.g. GitHub). See the Nature Research guidelines for submitting code & software for further information.

Data

Policy information about availability of data

All manuscripts must include a data availability statement. This statement should provide the following information, where applicable:

- Accession codes, unique identifiers, or web links for publicly available datasets
- A list of figures that have associated raw data
- A description of any restrictions on data availability

The data supporting the findings in this study are available from the corresponding author upon reasonable request.

Field-specific reporting

Please select the best fit for your research. If you are not sure, read the appropriate sections before making your selection.

☒ Life sciences ☐ Behavioural & social sciences ☐ Ecological, evolutionary & environmental sciences

For a reference copy of the document with all sections, see nature.com/authors/policies/ReportingSummary-flat.pdf

Life sciences study design

All studies must disclose on these points even when the disclosure is negative.

Sample size	No statistical methods were used to pre-determine sample sizes but our sample sizes are similar to those reported in previous publications (References: Fritz et al., (2003) Nat Neurosci 6:1216–1223. doi:10.1038/nn1141, Fritz et al. (2010) Nat Neurosci 6:1216–1223. doi:10.1038/nn.2598, Atiani et al. (2014) Neuron 82:486–499. doi:10.1016/j.neuron.2014.02.029).
Data exclusions	In population PSTH averages we excluded neurons that had no significant auditory responses in any presentation of task sounds, in both passive and active conditions. This criterion was pre-established.
Replication	In multiple recording sessions (n=713) in multiple animals (n=32), we placed electrodes acutely in the brain and, by measuring their position with respect to permanent landmarks in the implant, stereotaxic coordinates, and neurophysiological markers such as tonotopic map position, we were able to ascertain the cortical areas (A1, dorsal PEG, VPr, dorsolateral frontal cortex) in which we were recording. We were subsequently able to confirm these cortical areas with neuroanatomical and histological analysis of the electrode paths and electrolytic marks made in the recording sites. We recorded from multiple neurons in each area (see Methods and Figures 2 and 4) and found that the responses of these neurons were consistent within area. As shown in Figure 2, we recorded many different cells from each area (n=2740 in A1, n=1337 in dPEG, n=658 in VPr) in passive listening conditions and found highly consistent and replicable responses that were distinctive for each area. We also recorded responses in the behaving animal, as shown in Figure 4 from multiple areas in many animals and recorded from A1 (n=71), dPEG (n=199), VPr (n=266), dlFC (n=138) and also found consistent responses from all neurons in these different areas, that were distinct from responses of neurons in the different areas. In this way, we were able to replicate successfully our conclusions about response properties of neurons in each of the four different cortical areas that we studied. replicated the recordings in many animals and in both hemispheres.
Randomization	Animal subjects (female ferrets) were randomly chosen from the colony for experimentation. Some animals were directly implanted with headposts for naïve neurophysiological recordings. Other animals were trained on auditory tasks and were implanted with headposts and used for behavioral neurophysiological recordings.
Blinding	No blinding was used in the study, as is common in behavioral neuroscience. However, all analyses of neural responses were conducted in the same way for all data acquired over a period of ~15 years in our laboratory, including data from multiple animals and investigators. The neuroanatomical studies were conducted by a researcher who was not directly involved in behavioral or neurophysiological studies, and received brains to process and during histological processing was blind to each animal history.

Reporting for specific materials, systems and methods

Materials & experimental systems	
n/a	Involved in the study
☒	☐ Unique biological materials
☒	☐ Antibodies
☒	☐ Eukaryotic cell lines
☒	☐ Palaeontology
☐	☒ Animals and other organisms
☒	☐ Human research participants

Methods	
n/a	Involved in the study
☒	☐ ChIP-seq
☒	☐ Flow cytometry
☒	☐ MRI-based neuroimaging

Animals and other organisms

Policy information about studies involving animals; ARRIVE guidelines recommended for reporting animal research

Laboratory animals	All animals used in this study were adult (1-4 years old) female ferrets (Mustela putorius furo) obtained from Marshall BioResources. Animals were spayed and descented. During behavioral studies, animals were placed on a water schedule to motivate them to perform the tasks, in which they received water as reward.
Wild animals	The study did not involve wild animals.
Field-collected samples	The study did not involve samples collected from the field.